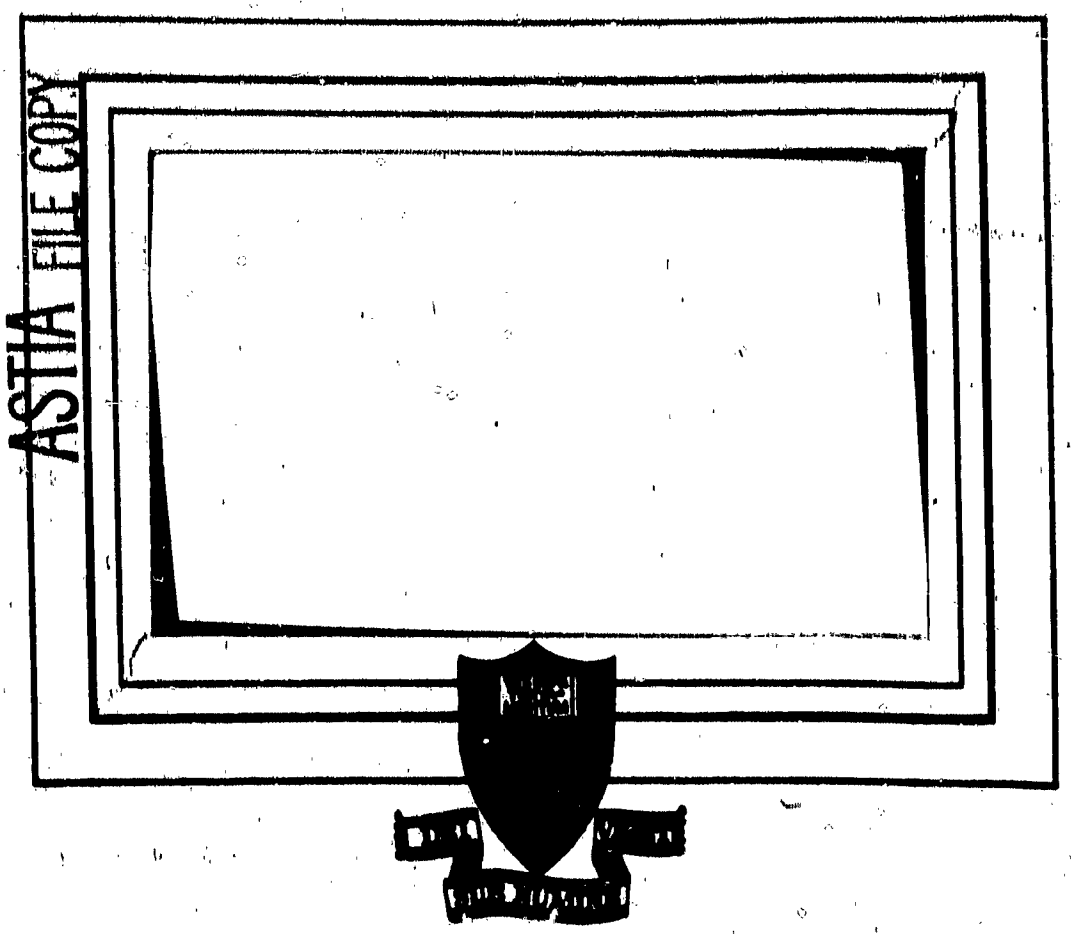

PRINCETON UNIVERSITY

DEPARTMENT OF AERONAUTICAL ENGINEERING

DEPARTMENT OF THE NAVY
BUREAU OF AERONAUTICS

Contract NOas 53-817-c

COMBUSTION INSTABILITY

IN

LIQUID PROPELLANT ROCKET MOTORS

Seventh Quarterly Progress Report

For the Period 1 November 1953 to 31 January 1954

Aeronautical Engineering Report No. 216-g

Prepared by _____
J. Grey, Research Engineer

Approved by _____
for L. Crocco, Professor in Charge

1 March 1954

PRINCETON UNIVERSITY
Department of Aeronautical Engineering

CONTENTS

I. SUMMARY

Shakedown operation of the bipropellant rocket motor at 300 psi chamber pressure was completed. Steady-state tests were run at mixture ratios from .95 to 1.3, and satisfactory operation was achieved. Minor modifications and revisions necessary included addition of an automatic cutout for the squib igniter and safety fuse, and installation of a pump-pressurised nozzle coolant system to replace the unsatisfactory shop-water system used on the shakedown series of tests. A detailed breakdown of the results of the first eighteen test runs is included later in the report.

The bipropellant flow modulating unit has been checked satisfactorily at speeds up to 12,000 RPM (200 cycles per second) under pressure conditions corresponding to those at 300 psi chamber pressure. The monopropellant unit, with a 1½ HP interim motor replacing the 3/4 HP drive originally used, has been checked satisfactorily up to 160 cycles per second under typical pressure conditions.

The major effort during this report period was concentrated on the instrumentation refinement program. Redesign and development of the cathode followers used to record mean values of the oscillating pressures on recording potentiometers culminated in an overall accuracy of ± 0.2%. Further refinements and modification to calibration techniques used in the 1d-1du pressure pickups have been successful in obtaining consistent results with errors of the order of ± ½% of full scale. Calibrations of the transient data recording system now under way indicate that accuracy levels are attainable which are appreciably better than have been heretofore achieved.

A complete revision of the central recording room facilities has been made, providing such features as universal patch-panel hookups, 100%

coaxial cable connections throughout, regulated power supplies, stable DC filament power supply, and proper signal ground provisions. Careful attention to details of this type has reduced the pressure pickup signal noise level by a factor of from ten to thirty, with comparable improvements in other circuit features.

II. INTRODUCTION

A. Object

BuAer Contract NOas 52-713-c was undertaken as a part of the jet propulsion research program of the Department of Aeronautical Engineering at Princeton to "conduct an investigation of the general problem of combustion instability in liquid propellant rocket engines." This program shall consist of theoretical analyses and experimental verification of theory. The ultimate objective shall be the collection of sufficient data that shall permit the rocket engine designer to produce power plants which are relatively free of the phenomena of instability. Interest shall center in that form of unstable operation which is characterized by high frequency vibrations and is commonly known as "screaming."

B. History

Interest at Princeton in the problem of combustion instability in liquid propellant rocket motors was given impetus by a Bureau of Aeronautics symposium held at the Naval Research Laboratory on the 7th and 8th of December 1950. This interest resulted in theoretical analyses by Professors M. Summerfield and L. Crocco of this Center.

Professor Summerfield's work, "Theory of Unstable Combustion in Liquid Propellant Rocket Systems" (JARS, September 1951), considers the effects of both inertia in the liquid propellant feed lines and combustion

A constant rate monopropellant feed system was designed and preliminary designs of the ethylene oxide rocket motor and the instrumentation systems were worked out. Special features of the projected systems included a flow modulating unit to cause oscillations in propellant flow rate, a water-cooled strain-gage pressure pickup designed for flush mounting in the rocket chamber, and several possible methods for dynamic measurement of an oscillating propellant flow rate.

Searches were made of the literature for sources of information on combustion instability and ethylene oxide, and visits to a number of activities working on liquid propellant rocket combustion instability problems were made for purposes of familiarization with equipment and results.

The basic precepts of Crocco's theory for combustion instability were reviewed, and detailed analyses made for specific patterns of combustion distribution.

Operational tests and calibration of the Princeton-MIT pressure pickup proved the value of the design, although failure of the pickup under "screaming" rocket conditions showed the necessity for modification of the cooling system.

Construction of the monopropellant test stand and rocket motor was completed. Modifications were made to the Princeton-MIT pressure pickup to provide for higher permissible heat-transfer rates in order that it be satisfactory for use under "screaming" conditions in a bipropellant rocket motor. Construction and preliminary testing of the hot-wire flow phasemeter and its associated equipment were completed.

A new contract, NOas 53-817-c, dated 1 March 1953, was granted by the Bureau of Aeronautics to continue the program originally started under

NOas 52-713-c. Operation of the monopropellant rocket motor was begun under this new contract, and shakedown operations were completed. It was found that decomposition of ethylene oxide could not be attained with the original motor design despite many configuration changes, and it was decided to avoid a long and costly development program by operating the "monopropellant" motor with small amounts of gaseous oxygen. The required limits of oxygen flow rate were determined at several chamber pressures, and it was demonstrated that the oxygen would probably have a negligible effect on performance when compared to the effect of ethylene oxide flow rate modulation. Preliminary tests with flow rate modulation up to 100 cps were performed for the purposes of system checkout, using interim AC amplifiers in lieu of the necessary DC instruments.

The time constant of the hot-wire liquid flow phasemeter was found to be 0.15 milliseconds and preparations for instantaneous flow calibrations were made. A test rig was constructed for this purpose.

A bipropellant rocket system using liquid oxygen and 100% ethyl alcohol was designed on the basis of monopropellant operational experience, incorporating an adjustable-phase flow modulating unit on both propellants. Injector design was based on a configuration used extensively by Reaction Motors, Inc.

Operation of the monopropellant system was performed with flow modulation at frequencies up to 120 cps, using a composite instrumentation system to measure mean values, amplitudes of oscillation, and phase difference between injector and chamber pressures. Analysis of the results of this program demonstrated approximate adherence to the pressure-time lag relationship used in Crocco's original theoretical treatment. Accuracy of the measurements was not adequate to provide a detailed check of the

theory, however, so an instrument refinement and development program was initiated.

The Mittelman electromagnetic flowmeter proved unsatisfactory due to equipment malfunctions, and had to be abandoned as a possible means of measuring instantaneous flow rates. The Li dynamic flowmeter also experienced a number of mechanical failures, and it was decided to concentrate all flow-measurement effort on the hot-wire, which, of all flowmeters tested, appeared to show the most promising results.

Construction of the bipropellant test stand was completed and the stand was put in readiness for operation. Subsequent efforts are presented in detail in the present report.

III. THEORY

An analysis of the special case of high-frequency combustion instability with concentrated combustion and distributed time lag has been performed. Here, all propellant elements are assumed to burn at the same physical location in the chamber, but are assigned an arbitrary steady-state distribution of pressure-sensitive time lags. The fundamental result of the analysis is that distribution of the time lags has a stabilising effect on combustion as compared with the case in which both space and time lags are assumed uniform. This condition was previously found to exist for low-frequency instability.

Details of the analysis are included as Appendix A to the present report.

IV. APPARATUS

A. Monopropellant Rocket Motor

No testing was performed on this stand during the report period due to activity on the bipropellant system and the instrumentation development program. Repairs to the flow modulating unit were completed, and operation with the pump-pressurized lubrication system was satisfactory. Failure of the unit to exceed 125 cycles per second was traced conclusively to insufficient power of the U. S. Motors varidrive, and the manufacturer supplied a 1½ HP replacement as an interim measure until the original 3/4 HP stator could be rewound to supply 2 HP, which is the maximum rating for the existing frame. With the 1½ HP drive, speeds of 160 cycles per second were achieved at 850 psi line pressure, and it is estimated that the forthcoming 2 HP installation will extend this range up to 175 or 180 cps. This is considered entirely satisfactory for the next series of monopropellant test runs.

B. Bipropellant Rocket Motor

After completion of preliminary water flow and pressure checks, the liquid oxygen system was dried as completely as possible in the subfreezing winter temperature, and propellant flow checks were begun. It was discovered that the Potter flowmeter had been inadequately dried, and had to be baked dry before the tests could be completed. After satisfactory flow checks had been made, providing determination of the proper orifice size in the liquid oxygen precooling system and other operating information, checkout of the pyrotechnic igniter revealed that improper electrical isolation of the safety fuse after burnout caused the safety system to operate, preventing the propellant valve from opening. This was corrected by addition of a holding relay to lock out the entire igniter electrical

system once the safety fuse had opened the propellant valve, and satisfactory operation was achieved.

The first four five-second test runs were not entirely satisfactory in that rough burning was experienced. The exact nature of the combustion could not be determined, since no transient instrumentation was used during the shakedown runs in order to avoid possible damage to the sensing elements. It was believed, however, that the rough burning was caused by oxygen vaporization in the injector, and the liquid oxygen feed lines were insulated prior to the fifth test run. No evidences of rough burning or instability were evident on this run or on any test run thereafter.

These first four tests provided the balance of required operational data; e.g., the time necessary for precooling the liquid oxygen line, the proper setting of the time-delay safety cutout (operated by chamber pressure), etc., and a mixture-ratio curve at 300 psi chamber pressure was run, beginning at an oxygen-fuel ratio of .95 and increasing with each ten-second run up to a maximum of 1.3. It was discovered after Run 15, however, that the liquid oxygen precooling valve was leaking badly, and it was replaced. As a result, Run 16 indicated a marked improvement in performance, and a rerun of the mixture-ratio test data was begun. Operation was satisfactory until after Run 18, when inspection of the nozzle revealed a small burnout just downstream of the throat (See Figure 1). The cause of the burnout was traced to insufficient nozzle cooling water pressure, which had fallen to the neighborhood of 25 psi, one-third of the minimum requirement, during the run. Because of this unreliability in the shop water supply, it was decided to install a pump-pressurized nozzle coolant system. A spare nozzle, prepared in advance in case of such failure,

was installed, and a pump and motor of proper capacity were ordered. Testing will continue when the new nozzle coolant supply system has been completed.

The flow modulating unit has been operated satisfactorily up to 200 cycles per second at 600 psi line pressure, and is available for use in flow calibrations and rocket tests. Modulated flow operation will begin upon conclusion of the instrumentation refinement program discussed below.

A surplus vacuum-jacketed liquid oxygen storage tank and vacuum pump have been procured and installed. The only major service items still outstanding are the tank sight glasses for liquid-level determination in the alcohol and liquid oxygen propellant tanks.

C. Instrumentation

1. Pressure Pickups:

A complete history of the various Li-Liu pickups is presented here for review:

Differential Pickups:

Numbers 1, 2, 3, the original units, were fitted with the improved back-pressure seals, and had cooling passages modified for high heat transfer rates, but upon calibration were found to exhibit appreciable hysteresis and nonlinearity (over 2%). They were returned to the vendor for replacement of strain tubes and for diaphragm assembly modifications noted below.

Number 10 was one of the late model pickups, incorporating both improved back-pressure seals and modified cooling passages. It was sent to Bell Aircraft Corporation for vibration and acceleration tests after having been statically calibrated at Princeton. Upon its return, it was

found to be highly nonlinear, and was returned to the vendor for a new strain tube and diaphragm assembly modifications noted below.

Numbers 11 and 12, similar to Number 10, were used on approximately 40 monopropellant rocket test runs and numerous flow calibrations. Both pickups have performed satisfactorily on all occasions, and are available for continued use.

Numbers 13 through 16 are new pickups, identical to Numbers 11 and 12, except that tolerances on the safety-stop spacer ring have been tightened up to improve hysteresis characteristics. These pickups have not yet been calibrated.

Absolute Pickups:

Number 4 was burned out on a screaming rocket test at NACA, and was repaired and modified to increase allowable heat transfer rates. This modification was apparently successful, since no burnouts have since been experienced. After completion of repairs, Number 4 was returned to NACA for determination of temperature sensitivity in an electric furnace, at which time one of the strain-gage electrical connections failed. This has since been repaired, and the pickup is now on hand. Full safety overload stops were incorporated on the first repair.

Number 5 was used on hydraulic flow tests, and experienced mechanical buckling of the strain tube when exposed to water-hammer conditions. The strain tube was replaced, and the pickup used on a number of water flow calibrations. It was recently returned for installation of safety stops to prevent transmission of overloads to the strain tube.

Number 8 has been used on flow studies and on two bipropellant rocket tests. On the second test a strain-gage electrical connection failed, and the pickup was returned to the vendor for repairs and for

installation of safety stops.

Number 9 was used to take valid data on a screaming rocket motor at NACA. Mechanical buckling of the strain tube was encountered after the second test run, and the pickup was returned to the vendor for replacement of the strain tube and installation of safety stops.

Dummy Pickups:

Numbers 6 and 7 were both used on a number of heat-transfer tests on uncooled "screaming" motors at NACA. They are still available (at NACA) for additional testing of this type. These "dummies" have standard diaphragm, cooling and dimensional configurations, but do not possess strain tubes or electrical wiring.

Detailed hysteresis calibrations of the available pickups continued during the report period. Several of the pickups were found to be entirely satisfactory both on direct calibration and when calibrated with the improved mean-value recording system, producing an overall error not exceeding ½% of the differential range. However, not all pickups tested performed within these specifications. In particular, Pickups #1 and #3, which had been held to a linear range of approximately 200 psi, were found to exhibit appreciable nonlinearity as well as hysteresis, and were returned for installation of new strain tube assemblies as indicated above. Upon completion of forthcoming calibrations on Pickups #13 through 16, all differential pickups will be revised as necessary to duplicate the performance of #11 and #12, which exhibit the satisfactory accuracy mentioned above.

The acceleration tests performed at Bell Aircraft Corporation on Pickup #10 were not quantitatively conclusive; however, no deviation in zero signal was observed at shaker-table frequencies up to 2,000 cps

(approximately 12g maximum acceleration), and no effects of centrifugal accelerations up to 28g were observed. Considering the construction of the pickup, it is probable that acceleration effects will be negligible up to extremely high g-values, but some confirmation of this feature must eventually be obtained. One factor which must, however, be quantitatively checked with care is the temperature drift under typical rocket applications. Plans are now being made for determining this effect in both cooled and uncooled rocket chambers under stable and unstable conditions. It has also never been determined whether the diaphragm cooling provisions are satisfactory under "equilibrium" conditions of high-frequency instability, since the only available "screaming" data has been obtained on short, uncooled rocket runs with durations of the order of 8 seconds. This question will also be resolved by the use of cooled-motor tests.

2. Flowmeters:

Refinement of the hot-wire apparatus is continuing, with attention being focussed upon both probe and constant-temperature amplifier development. A new type of probe, which consists of a fiberglass filament coated with tungsten, has yielded much higher resistance (and hence sensitivity) than the original nickel wire, permitting a much smaller element to be used. Sensitivity tests have also revealed that an enormous increase in permissible wire temperature has been made possible by both the use of tungsten and the high flow pressures prevailing in the simulated rocket injection system, and a highly improved transient signal will be available in view of the resulting marked increase in probe sensitivity.

Modifications to the constant temperature feedback amplifier and other electronic components of the hot-wire flow phasemeter are in progress to correct electrical phase-shift in the desired range of operating

frequencies, and to level off the frequency-response curve at the low end, where initial testing will be performed. Dynamic checks of the probe and amplifier combination are expected to be made on the monopropellant stand during the next report period.

3. Recording System

For purposes of organizing the instrumentation refinement program, the recording system has been broken down into four sections: Mean-value recording, transient recording, phase-measurement, and general signal transmission and handling.

(a) Mean-value recording:

The two major items in this system are the Leeds and Northrup continuous recording potentiometers and the cathodefollowers used for isolating the mean pressure values from the transient portions of the signals. The major problems encountered in development of this combination were drift, hysteresis due to excessive electrical damping, nonlinearity, and ground currents, noise, etc. Drift was essentially eliminated by use of a balanced cathode follower output, no readable deviation being recorded in over two hours. The proper electrical time constant was reached by trial-and-error selection of resistors, achieving an optimum balance between stability and speed of response. Extraneous influences were recorded by grounding one inlet signal lead and using battery power supplies. The result was a stable D.C. level recording system which will properly average an oscillating signal to provide its mean value within ± 0.2% reading error.

Two channels of the final cathode follower design were constructed and checked out. A third channel is now under construction for the third pressure-pickup channel in the bipropellant system. Three fixed-range

recording potentiometers with 0-10 millivolt full-scale deflection are used with the cathode followers.

(b) Transient recording:

The basic items consist of a four channel constant-phase A.C. amplifier, a four-channel FM tape recorder, four channels of cathode follower for tape playback, and a recording magnetic oscillograph for ultimate viewing of the taped data. The only item so far dealt with has been the tape recorder, which has been adjusted and checked for proper operation of all components. The cathode followers have been designed and are now nearing completion in the electronics shop. This system will be checked out during the forthcoming report period.

(c) Phase measurement:

Two possible techniques have been considered, depending on the nature of the signal received from the modulated test runs. If the signals are suitable for low-pass filtering, it will be possible to measure an average phase shift over a number of cycles. This will be done by adjusting an R-C phase-shifting network until the two signals whose phase difference is to be measured form a straight-line Lissajous pattern on the oscilloscope screen, and reading the amount of phase-shift necessary to achieve this condition. This technique implies, however, that suitable low-pass filters can be constructed whose phase-shift and frequency response in the operating frequency range will be satisfactory. A set of M-derived filters with sharp cutoff settings of 70 cps, 170 cps, and 230 cps are now under construction; however, if these filters prove unsatisfactory from either a phase-shift or frequency response standpoint, several sections of an R-C filter can be easily constructed, the only disadvantage of the latter being the decreased sharpness of cutoff obtainable.

In case the signal is not amenable to filtering, a technique has been evolved whereby the phase difference between two non-sinusoidal signals can be measured at each instant and the output recorded continuously, thus supplying a point-by-point indication of the phase. This technique involves the creation of a pulse at the instant the value of an AC signal crosses zero, and measurement of the time between the incidence of two such pulses in the two signals whose phase difference is to be measured. Because of the increased complexity of measurement and analysis of this data, however, it is hoped that the raw signals will be of sufficient regularity to allow the filtering method to be used.

(d) Data transmission system:

Much of the inaccuracy as reported on previous data taken with the recording system used has been due to the introduction of spurious signals, high noise-level, and various other effects upon the transmitted signal. It was found, particularly in the system used for the pressure pickups, that improper grounding of the transmission line was responsible for a large number of circulating ground currents which have the effect of introducing appreciable hum into the receiving instrument. Furthermore, the use of a large number of plug-type connectors was responsible for high signal resistance in the long transmission lines. Inadequate shielding and grounding of the shields created still another increment of noise level which helped to reduce the overall accuracy of the signal.

The entire data transmission line system was reworked and rebuilt using coaxial cable wherever possible, reducing the number of plug connectors to an absolute minimum, and taking extreme care that the single-ended signal was grounded at one point and one point only; namely, at the receiving instrument ground bus. The pressure pickup power supplies and balancing

bridge circuits were revised to lower their overall impedance to ground, and therefore to cut down their stray hum pickup. It was found after the revised system was checked out that the overall RMS noise level was reduced from a value which formerly had varied anywhere from one to three or four millivolts down to a consistant value of less tha 1/10 of one millivolt. This latter noise level corresponds to a resolution of approximately 1 psi with a typical pressure pickup.

A complete revision was made of the central recording room facility. The new arrangement provides for universal patch-panel hookups in which any instrument may be applied to any sensing element in use in a matter of a few minutes. Coaxial cable connections were used throughout in order to reduce noise pickup and to maintain proper grounding of all signals. Initial experience with the new arrangement has indicated a marked improvement in operating efficiency and incidence of personnel errors as well as the previously mentioned improvement in electrical transmission characteristics.

V. INFORMATION AND DATA

1. Biprepellant System

A brief resume of the first eighteen test runs on the biprepellant test stand is presented here. Detailed results are summarized in Table I.

Runs Number 1, 2, 3, 4: These runs were all made for the purpose of obtaining operational data on the test stand itself. No instrumentation other than bourdon-type gages and Potter flowmeters were used for these runs, in order to avoid possible damage to the more delicate

sensing elements. Ignition was satisfactory, but none of the first four runs was allowed to extend to full term (10 seconds) because of appreciable combustion roughness of an irregular type. No detailed information on the character of this combustion is available because of the lack of instrumentation. The mixture ratios varied from about .8 to 1.1 on the four runs as recorded by Potter-type flowmeters.

Runs Number 5, 6, and 7: These runs were satisfactory in that proper insulation of the oxygen feed line eliminated the rough combustion noted on earlier tests. However, some of the minor mechanical features and operational instrumentation of the test stand did not operate exactly as required and consequently these runs were not entirely satisfactory.

Runs Number 8 through 15: These runs were all performed under apparently normal conditions at approximately 300 psi chamber pressure. The runs were of approximately 10 seconds duration. It was noted after Run 15, however, that the liquid oxygen precooling by-pass line was leaking rather severely, and this was repaired.

Runs Number 16, 17, and 18: These runs were made to recheck some of the points made on previous tests. It was found that performance was appreciably higher after the oxygen leak had been corrected, and consequently a new mixture-ratio curve was begun. After Run #18, however, inspection of the motor revealed that a small hole had been burned in the nozzle just down stream of the throat. (See Figure 1) As pointed out previously, this burnout was adjudged to improper nozzle coolant pressure.

The mixture-ratio curve is included in Figure 2, showing the marked improvement of the oxygen leak which had apparently existed up to and including Run #15. The mixture-ratio curve both for this pressure and for the 600 and 900 psi chamber pressures will be completed after delivery of the coolant pump and motor.

TABLE I

DETAILED ALCOHOL-OXYGEN PERFORMANCE DATA - RUNS #1-18

RUN NO.	CHAMBER PRESSURE (PSIG)	THRUST (LBS.)	MIXTURE RATIO (O/F)	Isp (SECONDS)	Isp (CORR. TO P_c=300)	DURATION (SECONDS)	COMMENTS
1	-	-	-	-	-	2.0	ROUGH COMBUSTION (NOT PLOTTED)
2	255	175	.71	146	150	5.2	ROUGH COMBUSTION (NOT PLOTTED)
3	268	187	.84	146	149	3.6	ROUGH COMBUSTION (NOT PLOTTED)
4	250	187	1.04	145	149	4.7	ROUGH COMBUSTION (NOT PLOTTED)
5	292	270	-	-	-	10.4	NO OX FLOW RECORDED
6	-	-	-	-	-	0.8	CHAMBER PRESSURE SAFETY SWITCH CUTOUT
7	205	280	1.15	196	208	10.4	PHOTO TAKEN TOO SOON (NOT PLOTTED)
8	333	300	.99	214	211	10.7	NORMAL
9	340	300	1.04	216	213	20.5	NORMAL
10	-	-	-	-	-	1.4	CHAMBER PRESSURE SAFETY SWITCH CUTOUT
11	292	258	.97	189	190	10.7	SEVERE FUEL LEAK (NOT PLOTTED)
12	312	269	1.11	190	189	5.6	SEVERE FUEL LEAK CORRECTED (NOT PLOTTED)
13	340	316	1.13	221	218	10.2	NORMAL
14	340	312	1.24	223	220	10.5	NORMAL
15	330	300	1.31	216	214	10.5	NOTED SEVERE OX LEAK CORRECTED SATISFACTORILY
16	307	290	.95	221	220	10.6	NORMAL
17	359	320	1.08	230	225	11.0	NORMAL
18	346	313	1.20	229	225	8.4	NORMAL- NOTED NOZZLE BURNOUT AFTER TEST

NOTE: $(Isp)_{corr} = Isp + .0866(300-P_c)$

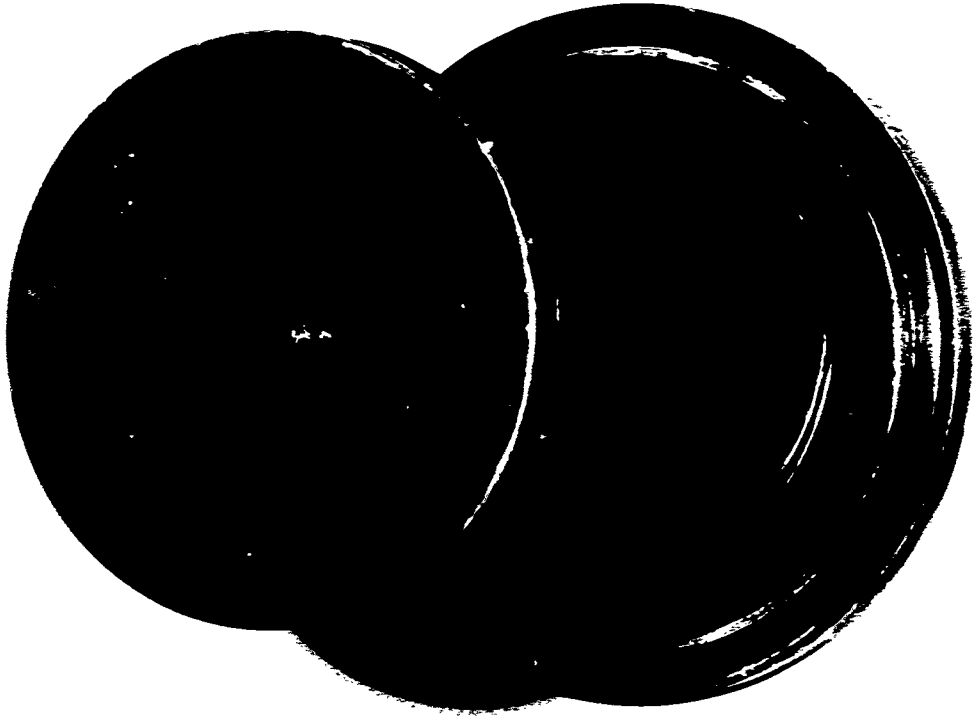

Figure I
Burnout of Bipropellant Nozzle after Run # 18
due to Insufficient Coolant Supply Pressure

Figure 2

Performance of alcohol-oxygen rocket motor as a function of mixture ratio

(P_c = 300 p.s.i.)

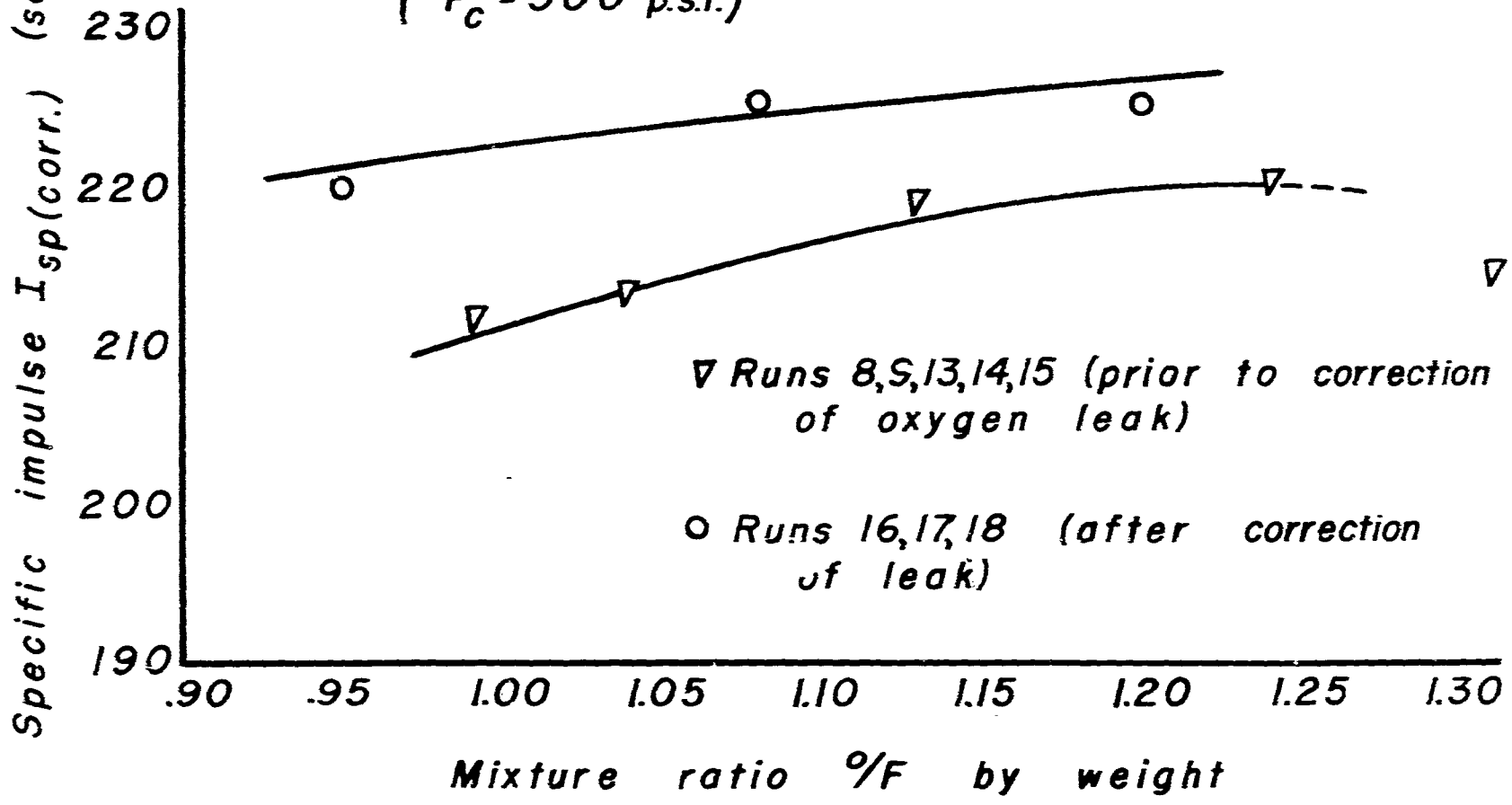

APPENDIX A

HIGH-FREQUENCY COMBUSTION INSTABILITY IN LIQUID PROPELLANT ROCKET WITH CONCENTRATED COMBUSTION AND DISTRIBUTED TIME LAG

LIST OF SYMBOLS

$\Theta/2 = L/c_o^*$	= characteristic time = time required for a sound wave to travel the entire length L of the combustion chamber filled with stagnant burned gas
$t = t^*/\frac{L}{c_o^*}$	= dimensionless time
$X = x^*/L$	= dimensionless length
$u, \bar{u} = u^*/c_o^*$	= velocity of the gas in unsteady and steady state operation nondimensionalized by the stagnation speed of sound
M	= Mach number of the gas flow
p, ρ, T	= instantaneous values of pressure, density, and temperature non-dimensionalized by dividing with their respective stagnation value
$\bar{p}, \bar{\rho}, \bar{T}$	= dimensionless steady state values of p, ρ and T.
p', ρ', T'	= dimensionless instantaneous perturbations over their respective steady state values
φ, δ, ν	= the time independent parts of pressure, density and velocity perturbations
τ_t	= dimensionless instantaneous value of the time lag reduced by the characteristic time $\Theta/2$
	$= \tau_i + \tau$
τ_i	= dimensionless value of the part of the total time lag which is insensitive to oscillations in combustion chamber
$\bar{\tau}, \tau$	= dimensionless steady state value and instantaneous value of the other part of the total time lag which is sensitive to oscillations in combustion chamber
τ_m	= arithmatic mean value of the maximum and the minimum values of the sensitive time lags of a group of propellant elements
$2\epsilon_o$	= fractional extent of the spread of the sensitive time lag
τ_e	= effective sensitive time lag of a group of propellant elements
c, c_1	= magnification factors of the effect of the spread of sensitive time lags defined in equation (2.13)
ξ	= dimensionless distance of the concentrated combustion front from the injector end expressed as a fraction of the characteristic length L

ξ_i = insensitive space lag = distance travelled by propellant element during insensitive time lag

n = exponent in the pressure dependence of the time lag = interaction index

n_{min} = minimum value of interaction index compatible with any unstable oscillations in a system

$\dot{m}_i$ = rate of injection of the propellant per unit cross sectional area of the combustion chamber

$\dot{m}_b$ = rate of the generation of the hot gas from the combustion of the propellant per unit cross sectional area of the combustion chamber

$\alpha (= \lambda + i\omega)$ = root of the characteristic equation with the dimensionless time as the independent variable

λ = dimensionless amplification coefficient

ω = dimensionless angular frequency

γ = adiabatic index of the combustion gas = c_p / c_v

β = reduced angular frequency of the oscillation

$I(\beta, \bar{u}) = \left[\frac{\bar{u}^2/\gamma}{\bar{\rho}/\beta}\right]_{\chi=1}$ = the specific acoustical admittance ratio of nozzle = the ratio of fractional variation of velocity to fractional variation of density at combustion chamber exit or entrance to nozzle

R, S = real and imaginary parts of $I(\beta, \bar{u})$.

h = integers characterizing discrete unstable range of the values of sensitive time lag for a given mode

K = integers characterizing the modes of the oscillation

Legend of Figures

Fig. 1 Specific admittance ratio I (β , $\bar{u}$) of a nozzle with linear steady state velocity in subsonic portion.

Fig. 2 The magnification factor of the effect of time lag spread: c_1 , linear distribution; c_2 , cosine distribution.

Fig. 3a The real part X of the expression defined in equation (3.1).

Fig. 3b The imaginary part Y of the expression defined in equation (3.1).

Fig. 4 Critical values of interaction index n for neutral oscillations of reduced frequency β . For systems with small time lag spread corresponding to c = 0.9.
a. Fundamental mode
b. Second mode

Fig. 5 Critical value of effective sensitive time lag for neutral oscillations of reduced frequency β for systems with small time lag spread corresponding to c = 0.9.
a. Fundamental mode
b. Second mode

Fig. 6 Stability diagram for systems with small time lag spread corresponding to c = 0.9, n = 1.00, u = 0.213, and γ = 1.20 plotted with effective sensitive time lag $\bar{\tau}_e$ vs. position ξ of concentrated combustion front.

Fig. 7 Minimum values of interaction index n compatible with any unstable oscillations vs. the magnification factor c of the time lag spread.

Fig. 8 Diagrams for graphical determination of stability boundary for systems with significant amount of time lag spread based upon equation (4.1)

Fig. 9 Critical values of interaction index n for neutral oscillations of reduced frequency β of the Fundamental mode with fractional extent of time lag spread ϵ_0 given as
(a). $\epsilon_0 = 1$ (b). $\epsilon_0 = 3/4$ (c). $\epsilon_0 = \frac{1}{2}$ (d). $\epsilon_0 = \frac{1}{4}$.

Fig. 10 Critical values of effective sensitive time lag $\bar{\tau}_e$ for neutral oscillations of reduced frequency β of the fundamental mode with fractional extent of time lag spread ϵ_0 given as
(a). $\epsilon_0 = 1$ (b). $\epsilon_0 = 3/4$ (c). $\epsilon_0 = \frac{1}{2}$ (d). $\epsilon_0 = \frac{1}{4}$.

Fig. 11 Stability diagram $\bar{\tau}_e$ vs. ξ for fundamental mode n = 1.00, h = 0, γ = 1.20 for systems with cosine type time lag spread of different fractional extent ϵ_0 .

Fig. 12 Minimum value of interaction index n compatible with any unstable oscillations vs. fractional extent ϵ_0 of time lag spread.

Fig. 13 Minimum value of interaction index n compatible with any unstable oscillations vs. position ξ of the concentrated combustion front for systems with different sensitive space lag $\xi = \xi_i$. Fundamental mode, no time lag spread and $\gamma = 1.20$.

Fig. 14 Minimum value of interaction index n compatible with any unstable oscillations vs. position ξ of the concentrated combustion front for systems with different sensitive space lag $\xi - \xi_i$. Fundamental mode with small time lag spread corresponding to $c = 0.9$ and $\gamma = 1.20$.

Fig. 15. Unstable ranges of the position of concentrated combustion front as defined by the values of ξ_e for systems with and without time lag spread $n = 1.00$. Fundamental mode.

1. Introduction

The stability of high frequency small longitudinal disturbances superposed on a combustion system in a liquid propellant rocket operating at normal or steady state has been investigated on a linearised basis in references 1, 2, and 3. It is found that the configuration of the combustion system especially concerning the spacewise and the timewise distribution of combustion elements is of considerable importance in determining the stability of the small disturbances. It has been pointed out in reference 4 that under the assumption of instantaneous combustion, the configuration of the combustion system can be schematically characterised by two distribution functions defining the "sensitive time lag" and the "total space lag" of propellant elements when the rocket is in steady state operation. The time lag is a scalar quantity while the space lag is a vector in general. In the simplified case of longitudinal oscillations, the space lag is also a scalar which is simply the distance from the injector end of the position where a propellant element is transformed into gaseous combustion products. Owing to the complexities of the mathematical formulation of the problem, previous treatments are only dealing with particular configurations. In references 1 and 2 all the propellant elements are assumed to have the same sensitive time lag and the same total space lag in steady state operation so that a concentrated or discontinuous combustion front is formed in the combustion chamber in both steady and unsteady state operation. In reference 3, the time lags of all the propellant elements are still assumed to be the same in steady state and the problem has been formulated for arbitrary space lag distribution while solution of the problem has been obtained only for the simplest extreme case of uniformly distributed space lags.

The present investigation is intended to look into the other extreme case where all the propellant elements are assumed to have the same total space lag but have arbitrary distribution of the sensitive time lag in steady state. In other words, we intend to consider a combustion system with concentrated combustion front where the propellant elements that burn at the concentrated combustion front at the instant t became sensitive at different instants $t - \bar{\tau}$ and in general at different distances from the injector end. The effect of spreading the sensitive time lag on the stability of low frequency disturbances was shown (1) to be always stabilizing. The result of the present investigation shows that the qualitative trend of the effect of spreading the sensitive time lag on the stability of high frequency disturbances in a given system is also stabilizing as compared to the corresponding system without time lag spread. The stabilizing effort of a given extent of time lag spread is more significant towards higher modes of oscillations and the stabilizing effect on a given mode of oscillation is larger if the extent of spread is larger.

The analysis of reference 2 for the systems with concentrated combustion front is made on the assumption that the sensitive time lag is of the order of unity so that all propellant elements sense the variations of the thermodynamic states of the burned gas only in the immediate neighborhood of the combustion front. When the sensitive time lag of an element is very large, the element will sense the chamber oscillations during its travel through a definite spatial range $\xi - \xi_1$ immediately upstream of the combustion front. The effect of such very large sensitive time lag and the effect of the spread of such large sensitive time lag are also treated briefly in the present paper.

2. Formulation and General Discussion

It is assumed in previous investigations that the propellant elements before being transformed into hot burned gas occupy little volume and hence do not contribute to the combustion chamber pressure of the whole system. The flow of the burned gas in steady state on both sides of the concentrated combustion front are not affected by the fact that the sensitive time lag of different propellant elements are different, provided that the rate of burned gas generation at the concentrated combustion front in steady state is the same. The description of the propagation of small disturbances upstream (region 1) and that downstream (region 2) of the concentrated combustion front are identical with those treated in Section 2 of reference 2. The only difference between the present treatment and that in reference 2 is the boundary condition at the concentrated combustion front $x = \xi$ where the solutions in region (1) and region (2) are joined together. With the same notation as was used in reference 2, the solutions in region 1 and region 2 are given by equations (2.5.2) and (2.5.6) in reference 2 as

$$\begin{cases} v_1(x) = c_{s_1} \exp(-\alpha a_s x)\left[1-\exp\left\{-\alpha(a_n - a_s)x\right\}\right] \\ \delta_1(x) = -c_{s_1} \exp(-\alpha a_s x)\left[1-\exp\left\{-\alpha(a_n - a_s)x\right\}\right] \end{cases} \tag{2.1}$$

and

$$\begin{cases} v_2(x) = c_{s_2} \exp(-\alpha a_s x)\left[1- B\exp\left\{\alpha(a_n - a_s)(1-x)\right\}\right] \\ \delta_2(x) = -c_{s_2} \exp(-\alpha a_s x)\left[1+ B\exp\left\{\alpha(a_n - a_s)(1-x)\right\}\right] \end{cases} \tag{2.2}$$

for region (1) and region (2) respectively. Here v is the velocity perturbation nondimensionalised by stagnation sound speed in the burned gas and δ is the

density perturbation nondimensionalized by stagnation density of the burned gas. The constant B is defined by

$$B(\beta, \bar{u}) = \frac{1 + I(\beta, \bar{u})\,\bar{u}}{1 - I(\beta, \bar{u})\,\bar{u}} \tag{2.3}$$

with I standing for the specific accoustical admittance ratio of oscillating gas flow through a deLaval nozzle. The specific accoustical admittance ratio is the ratio of the fractional velocity variation to the fractional density variation of the gas entering the nozzle. This admittance ratio depends on the reduced frequency β of the oscillation, the steady state gas velocity entering the nozzle and the geometry of the subsonic portion of the nozzle. The values of $I(\beta, \bar{u})$ for a nozzle with linear steady state velocity in subsonic part are reproduced from (5) as fig. 1. For this particular nozzle, the reduced frequency β is equal to the ratio of the angular frequency of oscillation and the steady state velocity gradient in the nozzle.

The first part of the boundary condition at the concentrated combustion front is still the continuity of the pressure and the density perturbations across the combustion front at any instant. The characteristic constant $\alpha = \lambda + i\omega$ is therefore also continuous. The second part of the boundary condition at $x = \xi$ concerns with the discontinuity across the combustion front of the velocity perturbation that is prescribed by the variation of the local burning rate due to the variation of the sensitive time lags of the propellant elements. Since the sensitive time lags of different propellant elements, unlike the case treated in reference 2, are different, we expect that the value of $\nu_2 - \nu_1$ in the present problem is different from $\nu_2 - \nu_1$ as given by equation (2.4.2) of reference 2. The distribution of the amount of propellant elements having different $\bar{\tau}$ will enter into the expression of $\nu_2 - \nu_1$.

The instantaneous value of the sensitive time lag τ of a given propellant element is related to its steady state value $\bar{\tau}$ in terms of the local gas pressure p at the position x' at the instant t' by the following integral relation as defined by Crocco (1).

$$\int_{t-\tau}^{t} p^n \left[x'(t'), t'\right] dt' = \text{Constant}$$

$$= \int_{t-\bar{\tau}}^{t} \bar{p}^n \left[x'(t'), t'\right] dt' \propto \bar{p}^n \bar{\tau} \qquad (2.4)$$

Here the integrand represents the local and instantaneous rate of activation and the constant value of the integral represents the total amount of activation energy that is required for the given element to start the instantaneous combustion.

The local rate of activation processes depend on a number of physical quantities such as the pressure, temperature, relative velocity of the surrounding burned gas and so forth. For small oscillations, all these physical quantities may be correlated and the local rate of activation can be expressed in terms of any one of these physical quantities. Following Crocco, the gas pressure acting on the unburned element is selected as shown in equation (2.4). The interaction index n therefore represents an average index of the extent of interaction between the combustion processes and the different oscillations of these physical quantities existing in the combustion chamber.

The total amount of activation energy that each propellant element would absorb before its combustion depends also on a number of factors and in particular the mixture ratio of this particular element. Owing to the nonuniformity of the atomization and the mixing processes and so forth, the total amount of activation energy as represented by the constant of the integral would be different for different propellant elements. In the cases of conventional

liquid rocket engines except for the throatless motor, the chamber pressure in steady state can be considered as uniform everywhere in the combustion chamber. Thus the constant value of the integral can be approximately evaluated to be $\bar{p}^n \bar{\tau}$ as shown in equation (2.4) That this constant value of the integral varies with different propellant elements means that the steady state value of the sensitive time lag varies with different propellant elements. The sensitive time lags of different propellant elements are therefore expected to scatter or spread in a certain region in the neightborhood of the mean value. The extent of spread is likely to be larger for bipropellant systems as compared to that for monopropellant systems.

Let $2\epsilon_0$ be the frational total extent of the spread of the sensitive time lags of the propellant elements; i.e. $\bar{\tau}_{max} - \bar{\tau}_{min} = 2\epsilon_0 \bar{\tau}_m$ with $\bar{\tau}_m = (\bar{\tau}_{max} + \bar{\tau}_{min})/2$. Let $f(\epsilon)$ be the amount of the propellant elements having sensitive time lags lying between $\bar{\tau} = \bar{\tau}_m (1+\epsilon)$ and $\bar{\tau}_{min} = \bar{\tau}_m (1-\epsilon_0)$ as a fraction of the total amount of the typical sample. Thus $f(\epsilon_0) = 1$ and $f(-\epsilon_0) = 0$. This definition of f coincides with the definition of the distribution parameter f defined in reference 1 in the treatment of the chugging or low frequency case. Since we are considering only instability of the intrinsic type where the rate of injection and the pattern of distribution of propellant elements are independent or insensitive to the oscillations in the combustion chamber, $f(\epsilon)$ is independent of time. The fractional amount of propellant elements having sensitive time lag lying between $\bar{\tau}$ and $\bar{\tau} + d\bar{\tau}$ is $\frac{df}{d\bar{\tau}} \cdot d\bar{\tau} = \frac{df}{d\epsilon} d\epsilon$ with

$$\int_{\bar{\tau}_{min}}^{\bar{\tau}_{max}} \frac{df}{d\bar{\tau}} d\bar{\tau} = \int_{-\epsilon_0}^{\epsilon_0} \frac{df}{d\epsilon} d\epsilon = 1 \qquad (2.5)$$

The rate at which propellant elements of this category is being transformed into burned gas is given as

$$\dot{m}_{b\bar{\tau}}(\bar{\tau})\,d\bar{\tau} = \dot{m}_i \cdot \left(\frac{df}{d\bar{\tau}}\,d\bar{\tau}\right)\cdot\left(1-\frac{d\tau}{dt}\right) = \dot{m}_i\cdot\left(\frac{df}{d\epsilon}\,d\epsilon\right)\left(1-\frac{d\tau}{dt}\right)$$

The total rate of burned gas generation $\dot{m}_b$ is obtained by integrating $m_{b\bar{\tau}}\,d\bar{\tau}$ over the complete range of $\bar{\tau}$,

$$\dot{m}_b = \int_{\bar{\tau}_{min}}^{\bar{\tau}_{max}} \dot{m}_{b\bar{\tau}}\,d\bar{\tau} = \dot{m}_i \int_{-\epsilon_0}^{\epsilon_0} \frac{df}{d\epsilon}\left(1-\frac{d\tau}{dt}\right)d\epsilon$$

The fractional variation of the rate of burned gas generation from the steady state value $\bar{\dot{m}}_b = \bar{\dot{m}}_i = \dot{m}_i$ is hence

$$\frac{\dot{m}_b-\dot{m}_i}{\dot{m}_i} = \int_{\bar{\tau}_{min}}^{\bar{\tau}_{max}} \frac{df}{d\bar{\tau}}\left[\left(1-\frac{d\tau}{dt}\right)-1\right]d\bar{\tau} = \int_{-\epsilon_0}^{\epsilon_0}\frac{df}{d\epsilon}\left(-\frac{d\tau}{dt}\right)d\epsilon \qquad (2.6)$$

Differentiating equation (2.4) with respect to t to obtain $\frac{d\tau}{dt}$, substituting this into equation (2.6) and replacing the instantaneous quantities by the sum of mean quantities and their respective perturbations of the exponential type, one obtains for equation (2.6) the following expression of the fractional burning rate perturbation

$$\frac{\dot{m}_b-\dot{m}_i}{\dot{m}_i} = \eta e^{-\alpha t}\int_{\bar{\tau}_{min}}^{\bar{\tau}_{max}}\frac{df}{d\bar{\tau}}\left\{\varphi(\xi)-\varphi\left[\xi_i(t-\bar{\tau})\right]e^{-\alpha\bar{\tau}}\right\}d\bar{\tau}$$

$$= \gamma\eta\, e^{-\alpha t}\left\{\delta(\xi)-\int_{-\epsilon_0}^{\epsilon_0}\frac{df}{d\epsilon}\,\delta\left[\xi_i(t-\bar{\tau})\right]e^{-\alpha\bar{\tau}}\,d\epsilon\right\} \qquad (2.7)$$

where φ is replaced by $\gamma\delta$ under the assumption of isentropic small oscillation and equation (2.5) has been introduced to obtain the last expression. Both $\frac{df}{d\epsilon}$ and $\bar{\tau} = \bar{\tau}_m(\epsilon)$ and the integrand are functions of ϵ. If $\delta(\xi)$ does not vanish, equation (2.7) can be rewritten as

$$\frac{\dot{m}_b-\dot{m}_i}{\dot{m}_i} = \gamma\eta\, e^{-\alpha t}\,\delta(\xi)\left[1-c_e\,e^{-\alpha\bar{\tau}_e}\right] \qquad (2.8)$$

with

$$C e^{-\alpha \bar{\tau}_e} = \int_{-\epsilon_0}^{\epsilon_0} \left(\frac{df}{d\epsilon}\right) \frac{\delta[\xi_i(t-\bar{\tau})]}{\delta(\xi)} e^{-\alpha\bar{\tau}} \, d\epsilon \qquad (2.9)$$

where C and $\bar{\tau}_e$ are real quantities.

Equating the expression of fractional increase of burning rate to the fractional increase of the difference of the mass flow rates across the concentrated combustion front, and introducing the exponential form of the small perturbations, one obtains

$$v_2 - v_1 + \bar{u}(1-\gamma_n)\delta_1 + \bar{u}\gamma_n \delta_1 \cdot C \exp[-\alpha\bar{\tau}_e] = 0 \qquad (2.10)$$

which prescribes the discontinuity of the velocity perturbation $v_2 - v_1$ across the concentrated combustion front.

If the concentrated combustion front is very close to the injector end where both the mean velocity and the velocity perturbation must vanish, the velocity perturbation v_1 immediately upstream of the combustion front must be much smaller than the velocity perturbation v_2 immediately downstream of the combustion front; i.e. $|v_1| << |v_2|$. In this particular case equation (2.10) becomes after dropping the subscripts 1 & 2

$$v + \bar{u}(1-\gamma_n)\delta + \bar{u}\gamma_n \delta C \exp[-\alpha\bar{\tau}_e] = 0 \qquad (2.11)$$

By substituting equations (2.1) and (2.2) into equation (2.10) and replacing $a_2 - a_1$ by 2 under the approximation that $\bar{u}^2 << 1$, we obtain the following characteristic equation

$$\frac{1}{\alpha}\left[\frac{1-\beta\exp[2\alpha(1-\xi)]}{1+\beta\exp[2\alpha(1-\xi)]} - \tanh\alpha\xi\right] = [(1-\gamma_n) + \gamma_n C\exp(-\alpha\bar{\tau}_e)] \qquad (2.12)$$

for the determination of the characteristic constant $\alpha = \lambda + i\omega$ of a system with concentrated combustion at the position ξ. Equation (2.12) is closely

analogous to equation (4.1.1) in reference (2). The only difference between the two is that the expression $\exp[-\alpha\tau]$ in equation (4.1.1) is replaced by $C\exp[-\alpha\tau_e]$ in the present case.

For the determination of the stability boundary or the neutral curves with $\alpha = i\omega$, c is the modulus and $\omega\tau_e$ is the effective phase angle of the complex integral of equation (2.9). Hence c represents the magnification or contraction factor of the effect of the time lag spread and τ_e represents the effective time lag that enters into the stability calculation of the combustion system with the particular distribution function f (ϵ) in question. Both c and τ_e in general depend on the type of the distribution function f (ϵ), the extent of spread $\tau_m \epsilon_0$, the position ξ of the concentrated combustion front and the frequency ω of the particular mode of neutral oscillation. Once the dependence of c and τ_e on these parameters have been found for a particular distribution of time lag, the determination of the stability boundary and the frequency of the neutral oscillation will follow in a manner closely analogous to the procedure given in reference 2.

Since during the sensitive time lag, the propellant elements are upstream of the combustion front, that is, in region (1), the value of $\zeta(\xi_1)$ and $\zeta(\xi)$ should be evaluated using equation (2.1). In general, ξ_1 is different from ξ, then the expression (2.9) would encounter some singularity when $\zeta(\xi) = 0$ which does occur when the combustion front is located at the node of the pressure oscillation in the combustion chamber. This is only introduced by the division by $\zeta(\xi)$ which is not at all necessary except for the purpose of convenience and comparison with those in reference (2). The case with $\xi_1 < \xi$ will be treated in the last section of the present paper.

We shall first consider the case where the value of the pressure sensitive time lag τ is of the order of unity as was treated in reference 2. Since the velocity of the unburned propellant elements approaching the combustion front is

small as compared to the small quantity $\bar{u}$ which is the velocity of the burned gas downstream of the front, we shall adopt the assumption, following reference (2) that $\xi_i(t-\bar{\tau}) = \xi$ and that $\frac{\delta(\xi_i)}{\delta(\xi)} = 1$. Equation (2.9) then becomes simply

$$c\, e^{-i\omega\tau_c} = \int_{-\epsilon_0}^{+\epsilon_0} \frac{df}{d\epsilon}\, e^{-i\omega\tau_m(1+\epsilon)}\, d\epsilon \qquad (2.13)$$

where α is replaced by $i\omega$ for the case of neutral oscillation. Then the only complex quantity involved in the integral of equation (2.13) is $e^{-i\omega\tau_m(1+\epsilon)}$ whose modulus is unity. From equation (2.4) we see that the integral of the modulus of the complex integrand is unity, therefore we conclude that for neutral oscillations, and for completely arbitrary distribution of $\bar{\tau}$, we must have

$$c \leq 1 \qquad (2.14)$$

If we write the integral of equation (2.13) as:

$$c\, e^{-i\omega\tau_c} = e^{-i\omega\tau_m}\left[\int_{-\epsilon_0}^{0} \frac{df}{d\epsilon}\, e^{i\omega\tau_m\epsilon}\, d\epsilon + \int_{0}^{\epsilon_0} \frac{df}{d\epsilon}\, e^{-i\omega\tau_m\epsilon}\, d\epsilon\right]$$

$$= e^{-i\omega\tau_m}\int_{0}^{\epsilon_0}\left[\frac{df}{d\epsilon}(-\epsilon)\, e^{i\omega\tau_m\epsilon} + \frac{df}{d\epsilon}(\epsilon)\, e^{-i\omega\tau_m\epsilon}\right] d\epsilon$$

Thus if $\frac{df}{d\epsilon}(-\epsilon) = \frac{df}{d\epsilon}(\epsilon)$, that is, if $\frac{df}{d\epsilon}(\epsilon)$ is a symmetric or even function of ϵ, the last integral for the case of neutral oscillation $\alpha = i\omega$, is real. In this case,

$$\begin{cases} \tau_c = \tau_m \\ c = 2\int_0^{\epsilon_0} \frac{df}{d\epsilon}(\epsilon)\cos(\omega\tau_m\epsilon)\, d\epsilon \end{cases} \qquad (2.15)^*$$

Even function of $\frac{df}{d\epsilon}(\epsilon)$ corresponds to odd function of $f(\epsilon)$ i.e. antisymmetric distribution of $f(\bar{\tau})$ with respect to $\bar{\tau}_m$ as was assumed in reference (1) while dealing with the low frequency case and $\bar{\tau}_m$ was used in the

* If the integral in equation (2.15) is negative, c should be taken as the absolute value of the integral and τ_c is not equal to τ_m but $\frac{\pi}{\omega} - \tau_m$.

place of $\bar{\tau}_\epsilon$ for such antisymmetric f ($\bar{\tau}$). The simplest examples of such symmetric $\frac{df}{d\epsilon}$ (ϵ) are

$$\text{(i)}\quad \frac{df}{d\epsilon} = \frac{1}{2\epsilon_0} = \text{constant} \qquad \text{with} \quad c_1 = \frac{\sin \omega \epsilon_0 \bar{\tau}_m}{\omega \epsilon_0 \bar{\tau}_m}$$

$$\text{(ii)}\quad \frac{df}{d\epsilon} = \frac{\pi}{4\epsilon_0} \cos \frac{\pi}{2} \frac{\epsilon}{\epsilon_0} \qquad \text{with} \quad c_2 = \frac{\cos \omega \epsilon_0 \bar{\tau}_m}{1 - \left(\frac{2\omega \epsilon_0 \bar{\tau}_m}{\pi}\right)^2} \qquad (2.16)$$

as are given in reference (1). For arbitrary symmetric function $\frac{df}{d\epsilon}$ (ϵ), the integral in equation (2.15) can be carried out analytically by expanding $\frac{df}{d\epsilon}$ into Fourier series and integrating term by term. The coefficients of the Fourier expansion should of course be properly normalized so that equation (2.5) is satisfied.

It is important to note that, for particular type of distribution function, the value of c depends not only on the manner of distribution f (ϵ) but also on the angular displacement $\omega \bar{\tau}_m \epsilon_0$ of the neutral oscillation during the time interval of half the extent of time lag spread. In other words, c depends on the ratio of the total extent of time lag spread $2\bar{\tau}_m \epsilon_0$ to the period of the oscillation T. The magnitude of c remains less than unity and approaches unity when ϵ_0 approaches zero as it should be. Furthermore the factor c could vanish for particular values of the time lag spread as compared to period of oscillation for each type of distribution. In equation (2.16) the value of c_1 for type (i) distribution vanishes when the total extent of time lag spread $2\bar{\tau}_m \epsilon_0$ equals the period of oscillation or any integral multiples of the period; and c_2 for type (ii) distribution vanishes when $2\bar{\tau}_m \epsilon_0$ equals any odd integral multiples of half period not less than three half of the period. Since ω is approximately integral multiples of π and $\bar{\tau}_m \epsilon_0$ is only subjected to the restriction that $\bar{\tau}_m \epsilon_0 \leq \bar{\tau}_m$, the situation that $c = 0$ is not impossible.

The magnitude of c is of considerable importance in the stability behavior of a given system as can be seen from the following qualitative consideration. In the case of intrinsic instability, the only excitation agent is the variation of

the specific rate of burned gas generation which is produced by the variation of the sensitive time lag. Equation (2.7) shows that this variation of gas generation rate can be divided into two parts, the first part is due to the pressure variation at the end of the time lag which is the same for all propellant elements burning simultaneously at the same location. The second part is due to the pressure variation that each element sensed in the beginning of its sensitive time lag. The contribution of the second part is different for different elements having different time lags even if they burn together. With optimum timing, the sum of the exciting contribution of the second part is added to that of the first part in stimulating instability. The modulus c represents the maximum amount of exciting contribution with optimum timing of the second part that is available to augment the excitation of the first part. Therefore, intuitively, we see that smaller values of c means a more stable system with optimum timing. The fact that c is in general less than unity (equation 2.14) when there is a spread of time lag indicates that the effect of the spread of time lag is always stabilizing so far as the unconditional stability is concerned. The stabilizing effect is maximized when c = o, that is when the increase of burning rate due to the pressure variations that a group of elements sensed in the beginning of their sensitive time lags is just balanced by the decrease of the burning rate due to that of another group of propellant elements. The qualitative result that a smaller value of c means a more stable system as obtained from the previous physical arguments is clearly verified by the calculated results given in later sections of the present paper.

Both C_1 and C_2 are plotted as shown in figure 2. From these two curves or from equation (2.16) directly we see that c is a damped oscillating function of $\omega\bar{\tau}_m$, ϵ_b and the magnitude of C is rather small compared to unity when $\omega\bar{\tau}_m$, ϵ_b is bigger than the first zero of the function C ; for example π

for c_1 and $\frac{3\pi}{2}$ for c_2. This situation can arise either when ω is large for higher modes of oscillation or when the total extent of the spread of time lag $2\bar{\tau}_m \epsilon_o$ is sufficiently large as compared to the period of oscillation. Therefore for a given fractional extent of spread ϵ_o, unstable ranges of the values of $\bar{\tau}_e$ or $\bar{\tau}_m$ corresponding to larger integral values of h for a given mode of oscillation is less likely. Also for given extent of time lag spread $\bar{\tau}_m \epsilon_o$, it is less likely that higher modes of oscillation corresponding to larger integral values of k could become unstable.

3. Systems with Small Time Lag Spread

Because of the dependence of C on ω and $\bar{\tau}$ the determination of stability boundary with time lag spread is slightly more complicated than that in reference 2. However if the total extent of the spread of the time lag $2\bar{\tau}_m \epsilon_0$ is sufficiently small compared to the period T of oscillation so that $\omega\bar{\tau}_m \epsilon_0$ is a small quantity for the fundamental or the first few higher modes, the value of c is nearly constant for each mode of oscillation and is close to but slightly less than unity. For such cases the determination of the stability boundary is considerably simplified with the approximation c = constant for all possible values of ω_* of the neutral oscillations of a given mode. The small variation of c due to the small variation of ω_* of the order of M can be neglected as higher order small quantity. In this section we shall first consider systems with small time lag spread.

For the determination of stability boundary, we put $\alpha = i\omega$ in equation (2.12) where ω is the frequency of neutral oscillation, call the complex quantity on the left hand side of equation (2.12) $X + iY$,

$$X + iY = \frac{1}{n}\left[\frac{1 - B\exp[2i\omega(1-\xi)]}{1 + B\exp[2i\omega(1-\xi)]} - \tanh i\omega\xi\right] \tag{3.1}$$

where B is given by equation (2.3) which is a function of the neutral frequency ω, the burned gas velocity $\bar{u}$ and the geometry of the nozzle. For given nozzle geometry and $\bar{u}$, the complex quantity $X + iY$ is a function of ω and ξ only, independent of the values of C and $\bar{\tau}_e$ which characterize the time lag spread. Therefore both X and Y can be calculated for a series of values of ξ and ω and plotted as shown in fig. 3, which can be used for the determination of stability boundary for arbitrary values of C and $\bar{\tau}_e$.

Equation (2.12) can be rewritten as the following two real equations

$$\begin{cases} \gamma_n C \cos \omega\bar{\tau}_e = \gamma_n - (1-X) \\ \gamma_n C \sin \omega\bar{\tau}_e = -Y \end{cases} \tag{3.2}$$

The critical values of the index n of interaction and of the effective sensitive time lag $\bar{\tau}_c$ corresponding to neutral oscillations of frequency ω are obtained as

$$n = \left\{ (1-X) - (1-X)C\left[1 - \frac{1-C^2}{C^2}\frac{Y^2}{(1-X)^2}\right]^{1/2} \right\} \Big/ \gamma (1-C^2) \qquad (3.3)$$

$$\bar{\tau}_c = \frac{1}{\omega} \sin^{-1}\left[\frac{-Y}{\gamma n C}\right] \qquad (3.4)$$

where the arc sine is taken in the gradrant consistent with the sign of $\cos \omega \bar{\tau}_c$ as given in equations (3.2).

If n is of the order of unity, equations (3.2) show that $|Y|$ must be of the order of unity because C is less than unity. An investigation of equation (3.1) leads to the conclusion similar to the case without time lag spread that $\sin \omega$ must be of the order of M, so that the dimensionless frequencies of unstable oscillations, if any, will be close to integral multiples of π with deviation of the order of M. In the present dimensionless scheme, oscillations with frequency equal to integral multiples of π correspond to organ pipe modes of pure acoustical oscillation in the combustion chamber. Since n must be real, the range of possible values of the frequencies of neutral oscillations is further restricted by equation (3.3) that

$$\frac{C^2}{1-C^2} \geq \frac{Y^2}{(1-X)^2} \qquad (3.5)$$

For a given system with given type of time lag distribution and the extent of its spread, C is a function of ω only. $\frac{Y}{1-X}$ is also a function of ω. Equation (3.5) then sets up both an upper and a lower limit of ω. When C vanishes the frequency ω of neutral oscillation is restricted to a single value ω_0, where $Y(\omega_0)$ vanishes. When C equals unity for systems without time lag spread, no such limits exist. Both these limits depend on the nature of the time lag spread and the configuration of the combustion distribution and of the nozzle.

As noted before, the factor C for given type of time lag spread with fixed $\frac{df}{d\epsilon}$ and ϵ_0 depends not only on the frequency ω of neutral oscillation but also on $\bar{\tau}_m$ which is the same as $\bar{\tau}_e$ for symmetric $\frac{df}{d\epsilon}$. Therefore, equations (3.3) and (3.4) do not give explicit solutions of n and $\bar{\tau}_e$ in general. But if the extent of time lag spread $\bar{\tau}_m \epsilon_0$ is sufficiently small so that $\omega \bar{\tau}_m \epsilon_0/\pi = \frac{2\bar{\tau}_m \epsilon_0}{T}$ is relatively small as compared to unity, and the variation of C for each mode of oscillation due to the small variation of ω is neglected, C can be assumed to be constant for a given mode of oscillation, and equations (3.3) and (3.4) give directly the critical values of n and $\bar{\tau}_e$ corresponding to different values of ω in the neighborhood of certain integral multiple of π. Since C is close to unity equation (3.3) can be expanded into a power series of $1-C^2$ as

$$n = \frac{1}{\gamma}\frac{1-X}{1+C}\left\{1+\frac{1+C}{2C}\frac{Y^2}{(1-X)^2}\left[1+\frac{1}{4}\frac{1-C^2}{C^2}\frac{Y^2}{(1-X)^2}+\cdots\right]\right\} \quad (3.6)$$

which reduces to $n = \frac{1-X}{2\gamma} + \frac{Y^2}{2\gamma(1-X)}$ when $C = 1$ for the case of no time lag spread as is given in (2). Equation (3.6) shows that the critical value of n with time lag spread ($c < 1$) is always larger than the critical value of n without time lag spread corresponding to the same frequency ω of neutral oscillation. For given value of C, the minimum value of n is given by:

$$n_{min} = \frac{1-X(\omega_0)}{\gamma(1+C)}$$

where ω_0 is determined by

$$Y(\omega_0) = 0$$

This minimum value is always bigger than $\frac{1-X(\omega_0)}{2\gamma}$ which is the minimum value of n without time lag spread. Typical computed results with $\omega = \beta\sqrt{\pi}$ & M = 0.213 for C = 0.90 and several values of $\bar{\tau}$ corresponding to different positions of concentrated combustion front is shown in figures 4 and 5. The unstable ranges

for the effective time lag $\bar{\tau}_e$ for systems with n = 1 are shown in figure 6 versus ξ where the dotted curves indicate the stability boundary for the case with no time lag spread. It is clearly seen that the unstable regions of $\bar{\tau}$ v.s. ξ for the case with time lag spread $C = 0.9$ lie entirely inside the unstable regions for the case without time lag spread $C = 1.0$. The effect of spreading the sensitive time lag is thus found to be stabilizing in every respect. From figure 2 , we see that for fundamental mode of oscillation half extent of the time lag spread, $\bar{\tau}_m \epsilon_0$, is approximately 1/3 and $\frac{1}{4}$ at $C = 0.9$ for the sinusoidal and for the linear distribution respectively. Thus, the total extent $2 \epsilon_0 \bar{\tau}_e$ of time lag spread is nearly two third to one half of the wave propagation time in the combustion chamber. The stabilizing effect with $C = 0.9$ as seen from figures 4 and 6 is not very important. The stabilizing effect will of course increase as C decreases when the extent of time lag spread increases slightly from the small value. The minimum value of n compatible with unstable oscillations with combustion concentrated at injector end for different values of C are given in figure 7 with n_{min} shown to be increasing steadily as C decreases. The curve is shown dotted when c is considerably less than unity, because the assumption of constant C is not valid in the solution of the characteristic value problem.

4. Systems with Significant Amount of Time Lag Spread

When the extent of time lag spread is not very small compared to the period of oscillation, the variation of c due to the small variation of ω in the solution of the characteristic problem is no longer negligible. The critical values of n and $\bar{\tau}_e$ corresponding to neutral oscillations of frequency ω must be solved simultaneously from equations (3.2) and the equation defining c for given type of time lag distribution. Let us consider the symmetric sinusoidal distribution where c is given as c_2 in equation (2.16). Then, for a given frequency ω of neutral oscillation, the critical value of $\omega\bar{\tau}_e$ is given by

$$\sin \omega\bar{\tau}_e = \left(\frac{1}{c_2} - \cos \omega\bar{\tau}_e\right) = \frac{-Y}{1-X} \tag{4.1}$$

with

$$c_2 = \frac{\cos \omega\bar{\tau}_e \quad \epsilon_0}{1 - \left(\frac{2\omega\bar{\tau}_e \quad \epsilon_0}{\pi}\right)^2} \tag{2.16}$$

The right hand side of equation (4.1), $-Y/(1-X)$, is determined only by ω for given position of concentrated combustion, and the left hand side of equation (4.1) is a function of $\omega\bar{\tau}_e$ and ϵ_0 only. Thus both sides of equation (4.1) can be plotted independently of each other as shown in figure 8. A graphical solution of the characteristic value problem based on equation (4.1) and figure 8 is found very convenient. For neutral oscillation of frequency ω with given value of ξ, the value of $-Y/(1-X)$ is read from the left hand side curve. Then carry this ordinate to the right hand side curve for the selected value ϵ_0 and read the critical value of $\omega\bar{\tau}_e$ from the abscissa. When $\omega\bar{\tau}_e$ is determined, the critical values of $\bar{\tau}_e$ is immediately obtained by division and the critical value of n is obtained from

$$n = \frac{-Y}{\gamma c \sin \omega\bar{\tau}_e} = \frac{1-X}{\gamma(1-c\cos \omega\bar{\tau}_e)} \tag{3.8}$$

Typical computed results as given in figures 9 and 10 for systems with a nozzle having a steady state dimensionless velocity gradient $\overline{u}_x = \pi$ in its subsonic portion so that $\omega = \beta\pi$. Thus integral values of β indicate frequencies of pure accoustical oscillations. In figures 9 a, b, and c the critical values of n corresponding to neutral oscillations of different reduced frequency parameter β are given for systems with combustion concentrated at different positions Ξ and with different fractional extent ϵ_0 of time lag spread. In figure 10, the critical values of τ_e corresponding to neutral oscillations of different reduced frequency parameter β are given. All these curves are of similar shape as the corresponding curves without time lag spread given in figures 7 and 8 in reference 2 except that the curves with time lag spread are in general displaced toward larger values of n and smaller ranges of β. This obviously indicates the stabilizing effect of the time lag spread as compared to corresponding systems without time lag spread. In figure 11, the unstable regions of τ_e and Ξ for the fundamental mode of oscillation k = 1 and h = 0 with n = 1 are shown for different values of the fractional extent ϵ_0 of time lag spread of the sinusoidal type. The stabilizing effect of increasing ϵ_0 in reducing the unstable regions of the time lag τ_e and the position of the concentrated combustion front is clearly illustrated. This is due to the decrease of c with increasing extent of time lag spread $\tau_e\ \epsilon_0$. In figure 12, the minimum values of n for systems with combustion concentrated at the injector end are shown to be increasing with increasing fractional extent ϵ_0 of time lag spread of a given type. All these results confirm the stabilizing effect of the spread of the sensitive time lag.

Besides this stabilizing effect, there are also several other interesting aspects of the effect of the spread of time lag that are worth mentioning. In figure 9a with $\epsilon_0 = 1$, the value of n increases very fast from the minimum value, n_{min}, when β is smaller than $\pi - \tan^{-1} M.S\ (\omega)$ which corresponds approximately to n_{min}. The range of the frequencies of unstable oscillations does not extend very

far below the value of $\pi - \tan^{-1} M \cdot S(\omega)$ even when n is considerably larger than n_{min}. In figures 9b and 9c with $\epsilon_0 = 3/4$ and $\frac{1}{2}$ respectively, the same situation can be observed, but less significantly. That these must occur can be seen clearly from figure 8 that $\sin \omega\tau_c / (\frac{1}{\epsilon} - \cos \omega\tau)$ will not be more negative than certain value which corresponds to the smallest possible frequency of neutral oscillation of that mode. When ϵ_0 decreases corresponding to smaller fractional extent of time lag spread, the minimum value of $\sin \omega\tau_c / (\frac{1}{\epsilon} - \cos \omega\tau)$ extends further negatively. This results in a smaller frequency limit. When there is no time lag spread no such limits exist, the unstable oscillations with frequency much lower than the corresponding acoustical frequency could occur if the value of n of the propellant is sufficiently large. The existence of such a lower limit of the frequency of unstable oscillation has also been indicated in equation (3.5) where the limit is not very restrictive because of the small extent of time lag spread. Therefore, when the extent of time lag spread is comparable with the period of oscillation, the frequency of the unstable oscillation will not deviate significantly, from $k\pi - SM$ no matter how large the value of n may be.

The increasing stabilizing effect of larger extent of time lag spread of a given type leads to another interesting result that for a given value of n, and a given fractional extent ϵ_0 of time lag spread, the unstable range of τ_c for a given mode of oscillation at large integral values of h cannot exist, and that n_{min} increases with increasing h. Results of previous analysis with no time lag spread $\epsilon_0 = 0$, show that for a given mode of oscillation to become unstable, the pressure sensitive time lag can lie in any of the discrete ranges of values in the neighborhood of 2h + 1 where h takes successive larger integral values. The n_{min} of a given mode is independent of the value of h. When there is a given fractional extent ϵ_0 of time lag spread critical values of τ_c corresponding to successive larger values of h for a given mode lead to successive larger values

of $\omega\bar{\tau}_e \epsilon_o$ as well as $\omega\bar{\tau}_e$. Thus as a general trend, the increase of $\omega\bar{\tau}_e \epsilon_o$ results in the decrease in c (except for the oscillations of the values of C with decreasing amplitude). Therefore, when h takes larger integral values, the minimum value of n compatible with unstable oscillation of that mode is increased and the unstable region of $\bar{\tau}_e$ around 2h + 1 is reduced. For example, with $\epsilon_o = 1$ and n = 1, there is an unstable range of $\bar{\tau}_e$ around $\bar{\tau}_e \sim 1$ when h = 0, but there is no unstable ranges of $\bar{\tau}_e$ around $\bar{\tau}_e \sim 2h + 1$ when h = 1,2,3 etc.

The results as given in figures 11 and 12, and that in figure 7 for the case of small extent of time lag spread of any type, show rather conclusively that increasing extent of time lag spread stabilizes the combustion system primarily due to the decrease of c with increasing $\omega\bar{\tau}_m \epsilon_o$ or $2\bar{\tau}_m \epsilon_o$ /T. Since the magnitudes of c for the two types of time lag distribution depend only on the parameter $\frac{\omega\bar{\tau}_e \epsilon_o}{\pi} = \frac{\alpha\bar{\tau}_e \epsilon_o}{T}$, it can be easily inferred without further demonstration that, for a given extent of time lag spread, the stabilizing effect is larger for higher modes of oscillation, that is for oscillations of smaller period. This larger stabilizing effect of time lag spread toward higher modes of oscillations, like the larger stabilizing effect of the nozzle, helps in eliminating the unstable oscillations of higher modes.

Also in figure 12, the values of n_{min} are given for both the linear type and the sinusoidal type of time lag distribution. It is seen that n_{min} for linear type distribution is consistently larger than that for sinusoidal type. Since linear type distribution means that equal fractional amount of propellant elements are distributed in equal time lag interval, while the symmetric sinusoidal or the cosine type distribution indicates that more propellant elements are distributed near the mean value of the time lag, the result as shown in figure 12, therefore, indicates that a more uniform distribution is likely to have greater stabilizing effect. This last inference is, however, not conclusive since only two specific types of distribution have been investigated.

5. Systems with Large Pressure Sensitive Time Lag

It has been assumed in sections 3 and 4 that the sensitive time lag $\bar{\tau}$ is of the order of unity so that the insensitive space lag ξ_i is practically the same as the total space lag ξ and the definition of $ce^{-\alpha\bar{\tau}_c}$ with $\alpha = i\omega$ is given by equation (2.13) instead of equation (2.9). If now the sensitive time lag $\bar{\tau}$ is large, then ξ_i is in general slightly smaller than ξ and $\delta(\xi_i)$, which is the time independent part of the density variation of burned gas at ξ_i upstream of the concentrated combustion front is not the same as $\delta(\xi)$ at the front. The acoustical solution as given by equation (2.1) with $x = \xi_i$ should be used in evaluating $\delta(\xi_i)$. The quantity $\xi - \xi_i$ is the dimensionless distance travelled by the unburned propellant element during its sensitive time lag. The velocity of the unburned elements relative to the surrounding burned gas will be assumed to have been sufficiently damped out during the insensitive time lag so that the velocity of the unburned elements is approximately given by the mean burned gas velocity upstream of the concentrated combustion front. With the schematic representation of a concentrated combustion front, the burned gas velocity upstream of the front is negligibly small as compared to the burned gas velocity downstream of the front which is itself a small quantity M. The sensitive time lag $\bar{\tau}$ should be, at least, of the order of $\frac{1}{M}$ or larger in order that $\xi - \xi_i$ is not negligibly small compared to ξ. Therefore, if the total extent of the spread of the sensitive time lag of different elements is not very much bigger than unity, ξ_i of all propellant elements can be considered as equal and equation (2.9) defining $ce^{-\alpha\bar{\tau}_c}$ can be written as

$$c_1 e^{-i\omega\bar{\tau}_c} = \frac{\delta(\xi_i)}{\delta(\xi)} \int_{-\epsilon_0}^{\epsilon_0} \frac{df}{d\epsilon} e^{-i\omega\bar{\tau}(\epsilon)} \tag{5.1}$$

where c_1 is the magnification factor of the effect of the spread of sensitive time

lag with $\xi - \xi_i$ not negligible. The integral involved in equation (5.1) is the same as that in equation (2.13) defining $ce^{-i\omega\tau_e}$ for the case with pressure sensitive time lags of the order of unity i.e. $\xi_i = \xi$. The effect of large pressure sensitive time lag appears as a multiplying correction factor $\delta(\xi_i)/\delta(\xi)$, which is equal to $\cos \omega\xi_i / \cos \omega\xi$ for neutral oscillation of frequency ω. This multiplying correction factor is a real quantity. Therefore, for a given type of time lag distribution, the effective sensitive time lag is related to $\bar{\tau}_m$ and ϵ_o in the same manner no matter whether the magnitude of the sensitive time lag is of the order of unity or very large provided that the total extent of time lag spread is not too large. It is only the magnification factor that is modified by the ratio $\delta(\xi_i)/\delta(\xi)$ i.e. $c_1 = c\,\delta(\xi_i)/\delta(\xi)$. The characteristic equation (2.12) for the determination of the stability boundary remains unchanged with c_1 replacing c. The stability boundary can be determined in exactly the same manner as described in previous sections. From the results in previous sections, the larger the magnitude of c_1 is, the more unstable the system is. Therefore, the qualitative trend of the effect of large sensitive time lag on the unconditional intrinsic stability as expressed by the value of n_{min} compatible with any unstable oscillations, may be either stabilizing or destabilizing; because $\delta(\xi_i)/\delta(\xi)$ can be either larger or smaller than unity depending upon the values of ξ_i and ξ.

If all combustion is concentrated in the neighborhood of the injector, both ξ and ξ_i are approximately zero so that $\delta(\xi_i)/\delta(\xi) = \frac{\cos \omega \xi_i}{\cos \omega \xi}$ remains unity for whatever values of the sensitive time lag. The stability behavior of such a system is not affected by the order of magnitude of the pressure sensitive time lag for a given type of distribution of the time lag. If combustion is concentrated in the neighborhood of any anti-node of a given mode other than injector end, then $\cos \omega\xi_i / \cos \omega\xi$ is always less than or at most equal to unity.

Thus the system with $\xi_i < \xi$ is more stable than the system with $\xi_i = \xi$, everything else being the same. If combustion is concentrated in the immediate neighborhood of a node of a given mode, then $\cos \omega \xi_i / \cos \omega \xi$ becomes very large when $\xi_i < \xi$ while the limiting value of $\cos \omega \xi_i / \cos \omega \xi$ with ξ_i approaching ξ is unity. Thus the system with combustion concentrated at a pressure node is greatly destabilized by the large sensitive time lag. It is thus clearly seen that the effect of large sensitive time lag with ξ_i less than ξ depends not only on the position of the concentrated combustion front, that is the total space lag of the combustion system, but also on the different modes of oscillation that is being considered.

To illustrate this qualitative discussion, let us consider the unconditional intrinsic stability of the fundamental mode in systems with combustion concentrated at different axial positions. We shall restrict the present calculation to the case where the total extent of time lag spread $2\bar{\tau}_m \epsilon_0$ is sufficiently small so that

$$c_1 = \left| \frac{\delta(\xi_i)}{\delta(\xi)} \right| \cdot c$$

can be considered as constant for given values of ξ_i and ξ in the solution of the characteristic value problem. For this case the minimum value of n compatible with any unstable fundamental mode of oscillation is given by

$$n_{min} = \frac{1 - X(\omega_0)}{\gamma(1 + c_1)} \tag{5.2}$$

with

$$X(\omega_0) = \frac{-R(\omega_0)}{\cos^4(1-\xi)\omega_0 + (R^2+S^2)M^2 \sin^2(1-\xi)\omega_0 - 2SM \sin 2\omega_0(1-\xi)} \tag{5.3}$$

and ω_0 is obtained from $Y(\omega_0) = 0$ and can be determined from the following relation

$$\sin \omega_0 = -SM \frac{\cos(2-\xi)\omega_0}{\cos(1-\xi)\omega_0} + (R^2+S^2)M^2 \cos \omega_0 \tan(1-\xi)\omega_0 \tag{5.4}$$

For the fundamental mode, ω_0 is taken in the neighborhood of π, and both R and S are functions of ω_0 and the geometry of the deLaval nozzle. The present calculation is based on the values of R (ω) and S (ω) as given in figure 1 for a nozzle with a linear steady state velocity profile of dimensionless slope π in its subsonic portion and M_e is taken as 0.213.

Computed results for the fundamental mode of oscillation are shown in figures 13 to 15. In figures 13, the values of n_{min} are plotted versus the position ξ of the concentrated combustion front for several values of $\xi - \xi_i$ when there is no spread of the time lag i.e. C = 1. In figure 14, the same is plotted when there is a small spread of the time lag with C = 0.9. When combustion is concentrated at the injector end both ξ_i and ξ must vanish and the minimum value of n is not affected by large pressure sensitive time lag. The system with combustion concentrated at injector end is still the most unstable configuration that is the configuration with the smallest value of n_{min}. When combustion is concentrated in the upstream half of the combustion chamber, $\xi < \frac{1}{2}$, the value of n_{min} is decreased by large time lag and when combustion is concentrated in the downstream half, $\xi > \frac{1}{2}$, the value of n_{min} is increased by large time lag. By observing equation (5.2) that $X(\omega_0)$ is independent of ξ_i and of time lag spread, we see that the value of n_{min} is increased or decreased according as $|\delta(\xi_i)/\delta(\xi)| \leqslant 1$. Since ξ_i is less than ξ, the ratio $|\delta(\xi_i)/\delta(\xi)|$ is greater than unity when $\xi < \frac{1}{2}$ and the value of n_{min} is expected to decrease as shown in figures 13 and 14. The presence of time lag spread does not complicate the situation. This qualitative statement concerning the magnitude of the ratio of $|\delta(\xi_i)/\delta(\xi)|$ in determining the relative unconditional stability helps in understanding the effect of large time lag on the stability of higher modes of oscillation especially when $\xi - \xi_i$ is comparable with the wave length of that mode.

In figure 15, the critical values ξ_c that define the regions of the positions ξ of the concentrated combustion front where the fundamental mode is always stable when $n \leq 1$, are shown for different values of the pressure sensitive space lag $\xi - \xi_\lambda$. The stable region is seen to be shifted downstream as compared to the stable region when $\xi = \xi_\lambda$ and the magnitude of the shift increases when the pressure sensitive space lag becomes larger. For higher modes of oscillations the qualitative pictures of n_{min} v.s. ξ and the stable regions of ξ v.s. $\xi - \xi_\lambda$ in a half wave length are expected to be similar to those given in figures 13 to 15 for the fundamental mode, provided that $\xi - \xi_\lambda$ remains small compared with wave length. It should be noted, however, that so far as unconditional intrinsic stability of a system is concerned, the values of n_{min} of higher modes than the fundamental and/or the second mode are relatively of little importance because they are expected to be larger due to the increasing stabilizing effect of the nozzle toward higher modes of oscillations.

By comparing the values of n_{min} for given position of the concentrated combustion front ξ as given in figures (13) and (14) for $c = 1$ and $c = 0.9$ respectively, we see that the values of n_{min} with time lag spread ($c = 0.9$) is always the larger for any values of ξ_λ. In figure (15) the stable region for systems with $c = 1$, (without time lag spread) lies entirely inside the stable region for systems with $c = 0.9$, (with a small time lag spread). It is therefore concluded, that the stabilizing effect of distributing the time lag as compared to the corresponding system without time lag spread is not affected qualitatively by the order of magnitude of the sensitive time lag, be it of the order of unity, or of the order of $\frac{1}{M}$ or larger.

6. Summary of Conclusions

The stability of combustion in a liquid propellant rocket with combustion concentrated in a narrow region at distance ξ downstream of the injector end toward small high frequency disturbances are analyzed when the sensitive time lag of different propellant elements are distributed in a prescribed manner. Both the cases with dimensionless sensitive time lags of the order of unity and the cases with very large sensitive time lags of the order of $\frac{1}{M}$ or larger are treated. The effect of distributing the sensitive time lag can be represented by a magnification factor c defined by the following complex integral

$$c\, e^{-i\omega\bar{\tau}_c} = \int_{-\epsilon_0}^{\epsilon_0} \frac{df}{d\epsilon} \frac{s[\xi_i(t-\tau), t-t]}{s(\xi,t)} e^{-i\omega\bar{\tau}}\, d\epsilon$$

where c is the absolute magnitude of the complex quantity which represents the maximum possible amount of contribution in exciting instability due to the variation of burned gas pressure acting on different propellant elements at the beginning of their respective sensitive time lags. For a given geometrical configuration, the combustion is stabilized or destabilized by the spread of the time lag according as $c \lesseqgtr 1$. For different specific instances, the following conclusions are obtained:

1. When the sensitive time lag of the propellant is of the same order of magnitude as the time required for the pressure wave to travel the length of the combustion chamber, i.e. $\bar{\tau} = 0(1)$, the sensitive space lag $\xi - \xi_i$ is negligibly small. The magnification factor c is always less than or at most equal to unity when the sensitive time lags of different propellant elements are different. A system with time lags of different elements distributed in a certain region is more stable than the corresponding system with the same time lag for all propellant elements in having a larger value for n_{min} and smaller unstable regions of the time lag and the position of concentrate

combustion front for a given value of n of the propellant. The following conclusions numbered 2 to 5 pertain to systems with dimensionless time lag $\bar{\tau}$ of the order of unity.

2. When the extent of the time lag spread is considerably less than the period of oscillation of a given mode, the magnification factor c is only slightly less than unity and is nearly constant for a given type of time lag distribution and for a given mode of oscillation. When the extent of the time lag spread increases the magnitude of c decreases and the stabilizing effect increases even though the stabilizing effect remains small.

3. When the extent of the time lag spread is considerably larger than the period of oscillation either due to the small period of the higher modes of oscillation or due to the large extent of time lag spread, the magnitude of c is considerably less than unity, and these modes of oscillations are strongly stabilized by the spread of time lags. Thus higher modes of oscillation whose period is significantly less than the extent of the time lag spread is not likely to become unstable.

4. When the extent of the time lag spread is comparable to the period of oscillation, the stabilizing effect is quite significant and increases with increasing extent of time lag spread. The frequencies of unstable oscillations remain in the neighborhood of the corresponding acoustical frequency and will not be much lower than $k\pi - SM$ even when n is large.

5. For given extent of time lag spread which is small compared to period of oscillation, a system with propellant elements uniformly distributed in the range of time lag spread is more stable than a system with elements distributed according to consine law where more elements have time lags in the neighborhood of the mean value.

6. When the sensitive time lag of the propellant is much larger than the time required for the pressure wave to propagate the chamber length, i.e. $\bar{\tau} \gg 0(1)$ the qualitative stability behavior of the system is essentially similar to that of the corresponding system with $\bar{\tau} = 0(1)$, only that the stable regions about each node for given value of n are shifted downstream. For a given position ξ of the concentrated combustion front, the system with very large sensitive time lag is more stable or less stable than the corresponding system with sensitive time lag $\bar{\tau} = 0(1)$ according as $|\delta(\xi_i)/\delta(\xi)| \lesseqgtr 1$. The effect of spreading the pressure sensitive time lag on the stability of the system as compared to a corresponding system without time lag spread is in general stabilising as described in items 1 to 5 for the case when the dimensionless pressure sensitive time lag $\bar{\tau}$ is of the order of unity.

References

1. Crocco, L. "Aspects of Combustion Stability in Liquid Propellant Rocket Motors." Journal of American Rocket Society, Part II, vol. 22, No. 1, Jan. - Feb. 1952, p.p. 7-16.

2. Crocco, L. and Cheng, Sin-I. "High Frequency Combustion Instability in Rockets with Concentrated Combustion" presented at 8th Internation Congress of Applied Mechanics. Aug. 1952, Instanbul, Turkey. Published also in Journal of American Rocket Society, vol. 23, No. 5, Sept. - Oct. 1953.

3. Crocco, L. and Cheng, Sin-I. "High Frequency Combustion Instability in Rockets with Distributed Combustion." presented at 4th International Combustion Symposium, Sept. 1952, Boston, Mass. U.S.A. Published in the Proceedings of the Symposium.

4. Crocco, L. "Combustion Instability in Rocket Motors" delivered at Technical Meeting, AGARD, NATO, Dec. 1952, Roma, Italy.

5. Crocco, L. "Supercritical Gases Discharge with High Frequency Oscillations" L'Aero-tecnica vol. 33, No. 1, Feb. 1953. Special issue in honor of G. A. Crocco, text in English.

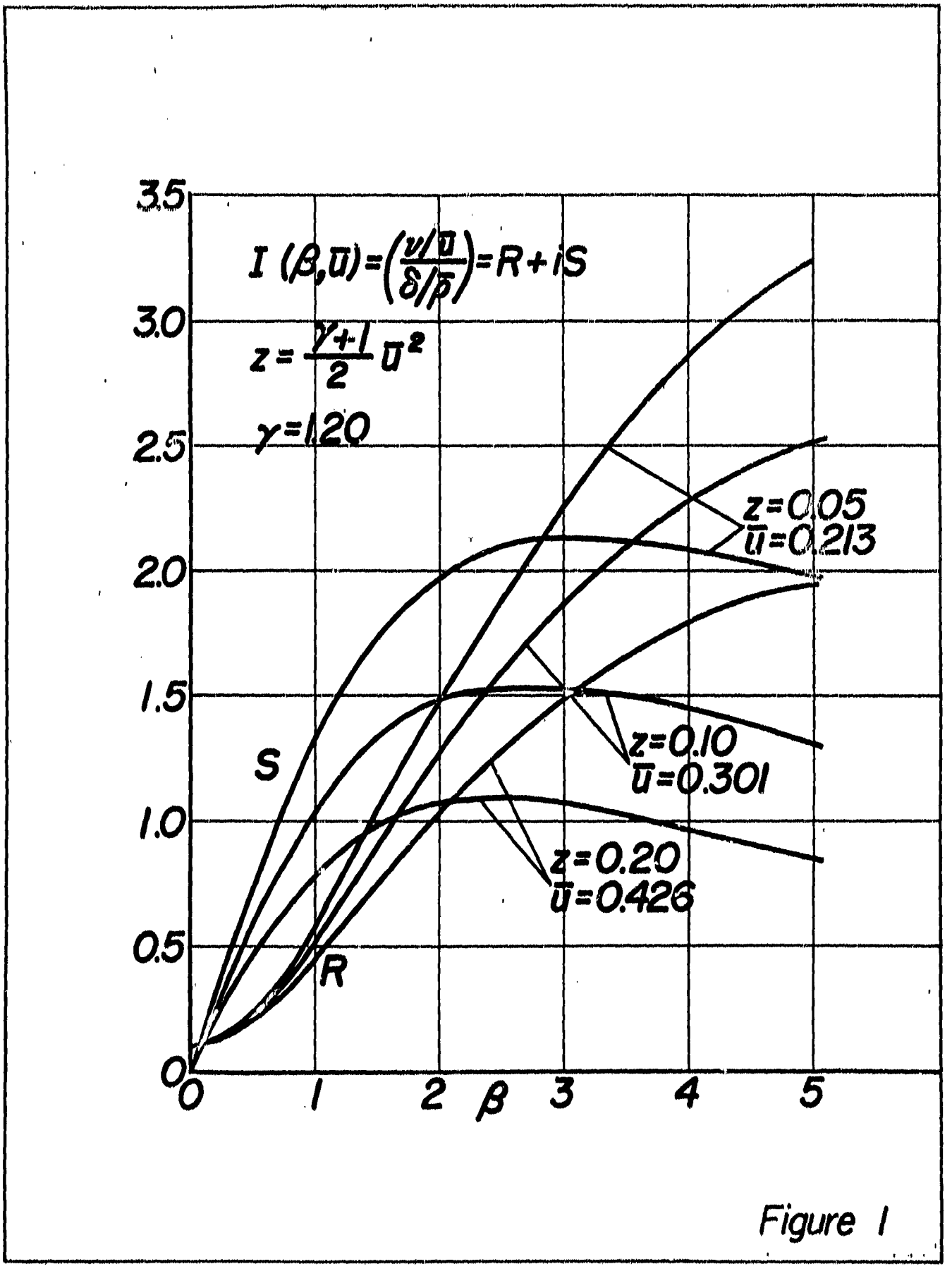
$I(\beta,\bar{u}) = \left(\frac{v/\bar{u}}{\delta/\beta}\right) = R + iS$
$z = \frac{\gamma+1}{2}\bar{u}^2$
$\gamma = 1.20$
z=0.05
ū=0.213
z=0.10
ū=0.301
z=0.20
ū=0.426
S
R
3.5
3.0
2.5
2.0
1.5
1.0
0.5
0
0
1
2
β
3
4
5

Figure 1

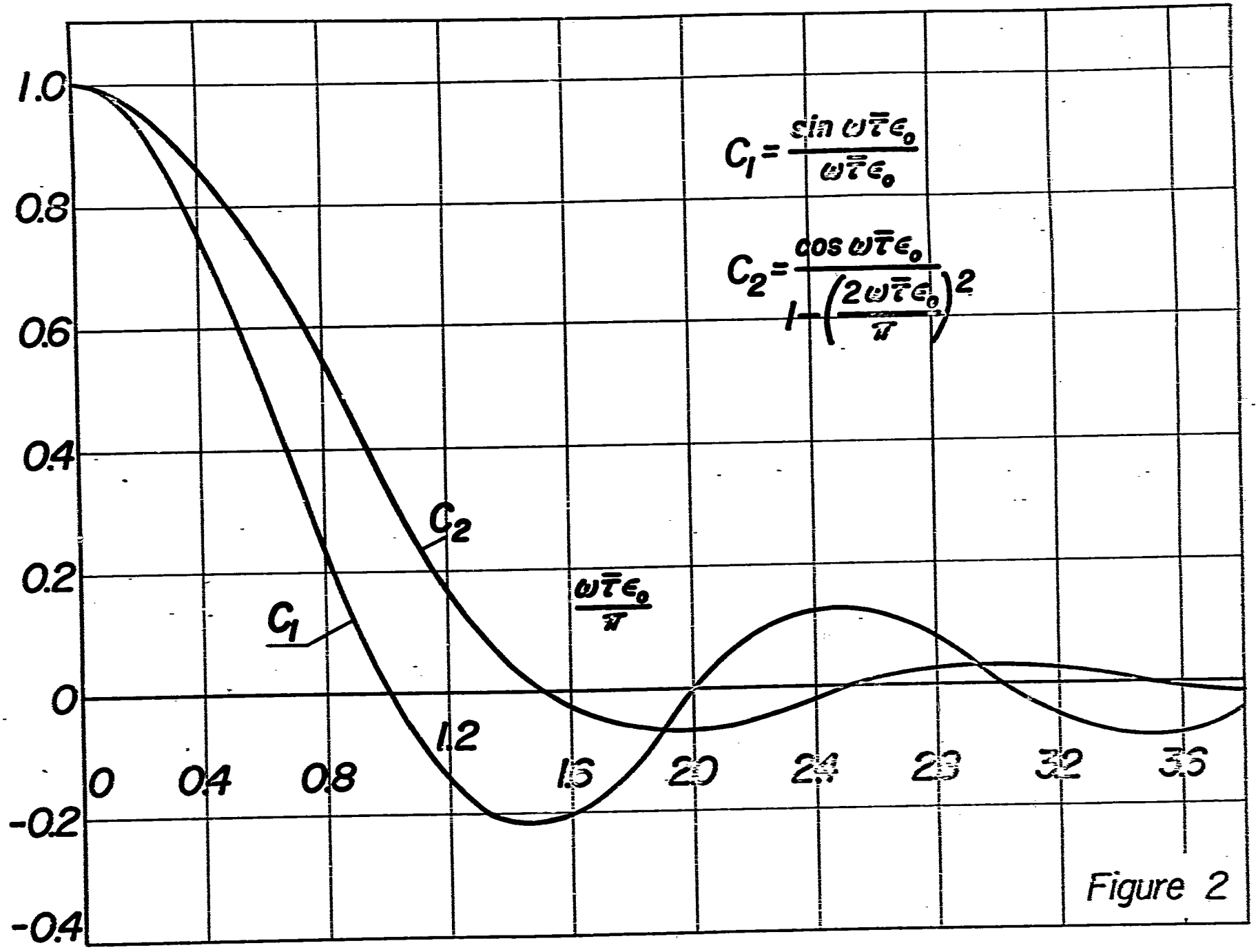
1.0
0.8
0.6
0.4
0.2
0
-0.2
-0.4
0
0.4
0.8
1.2
1.6
2.0
2.4
2.8
3.2
3.6
$C_1 = \frac{\sin \omega\bar{\tau}\epsilon_0}{\omega\bar{\tau}\epsilon_0}$
$C_2 = \frac{\cos \omega\bar{\tau}\epsilon_0}{1 - \left(\frac{2\omega\bar{\tau}\epsilon_0}{\pi}\right)^2}$
C_2
C_1
$\frac{\omega\bar{\tau}\epsilon_0}{\pi}$

Figure 2

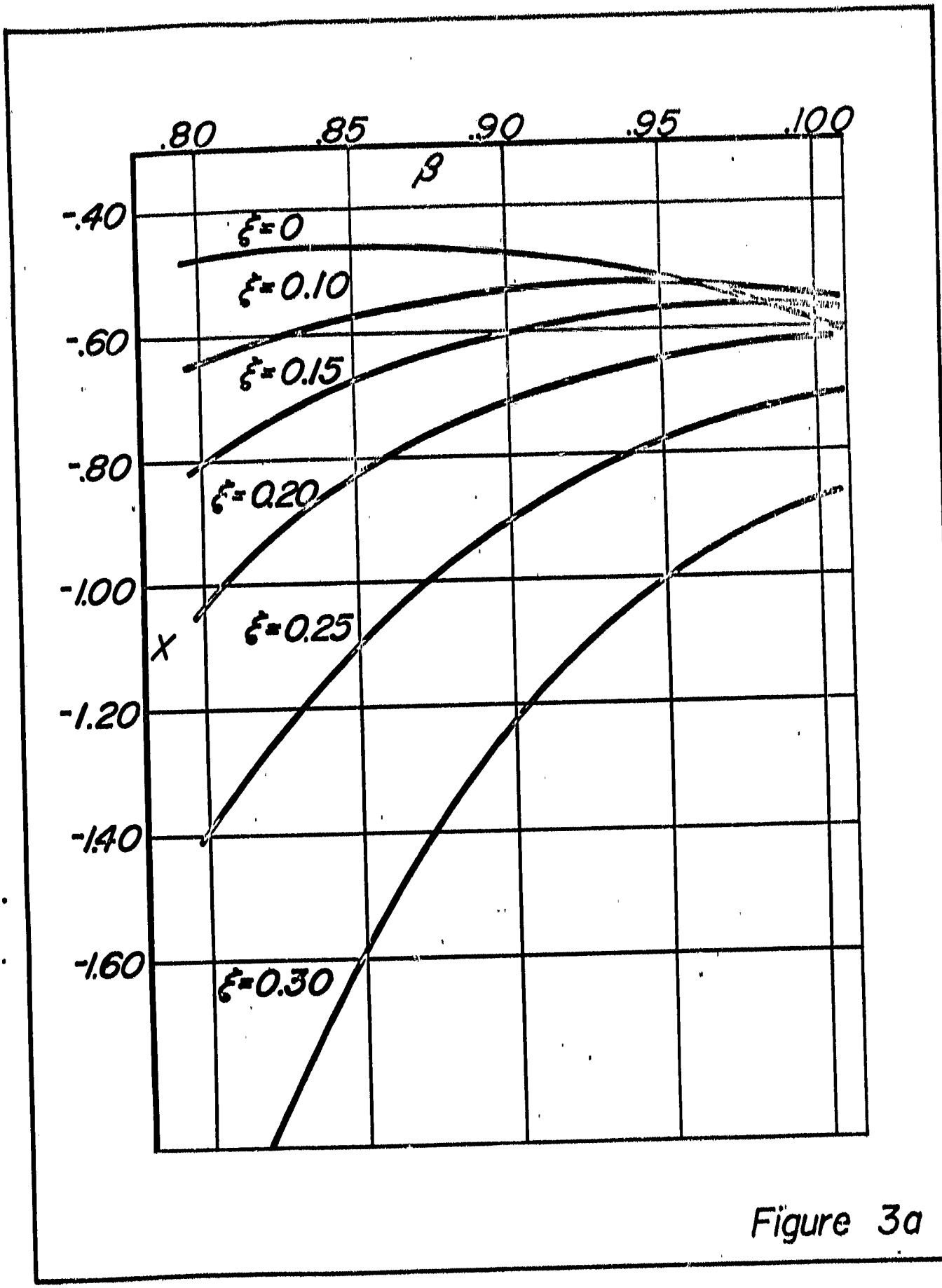
.80
.85
.90
.95
1.00
β
-.40
-.60
-.80
-1.00
-1.20
-1.40
-1.60
X
ξ=0
ξ=0.10
ξ=0.15
ξ=0.20
ξ=0.25
ξ=0.30

Figure 3a

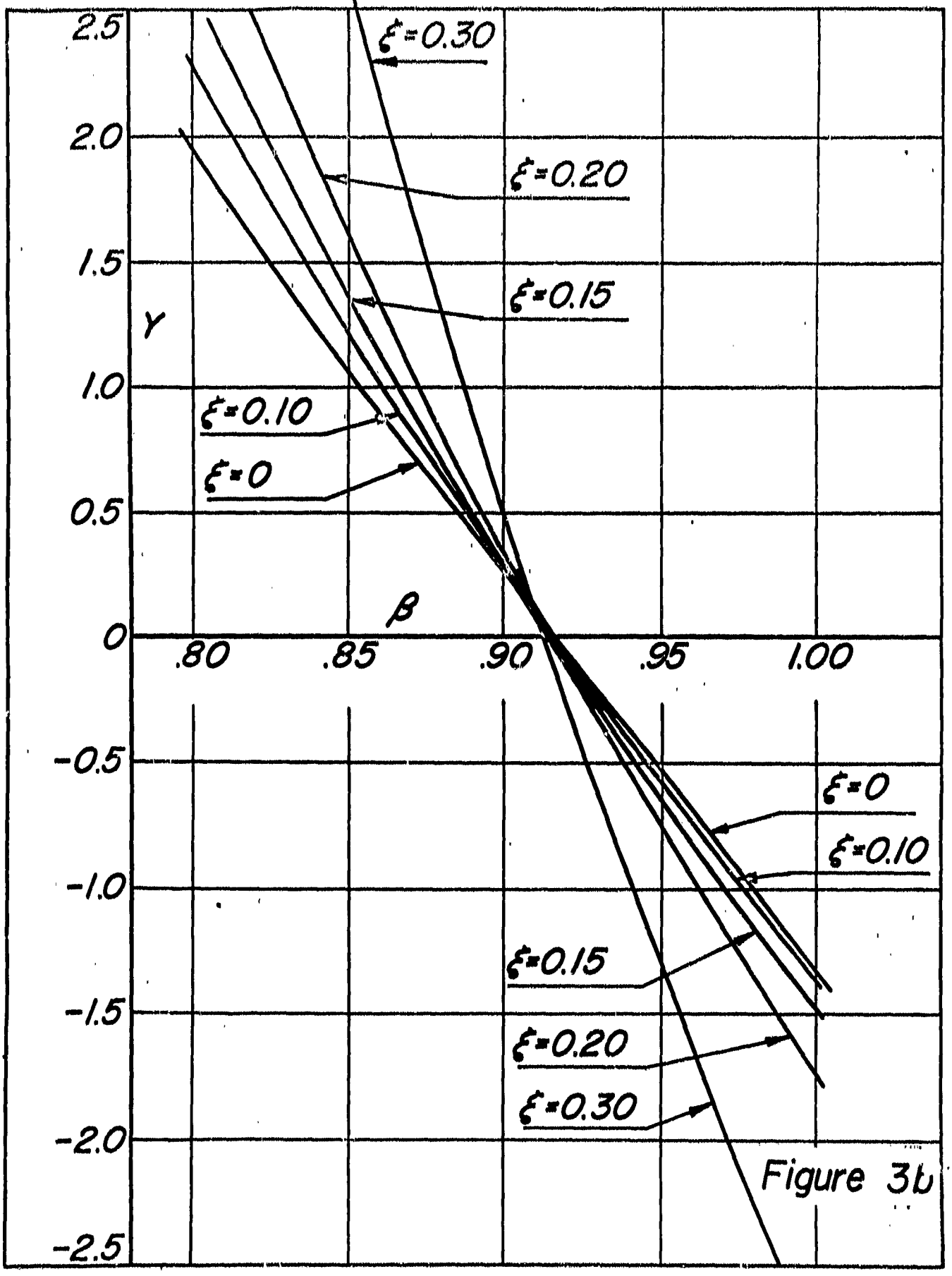
2.5
2.0
1.5
1.0
0.5
0
-0.5
-1.0
-1.5
-2.0
-2.5
Y
β
.80
.85
.90
.95
1.00
ξ=0.30
ξ=0.20
ξ=0.15
ξ=0.10
ξ=0
ξ=0
ξ=0.10
ξ=0.15
ξ=0.20
ξ=0.30

Figure 3b

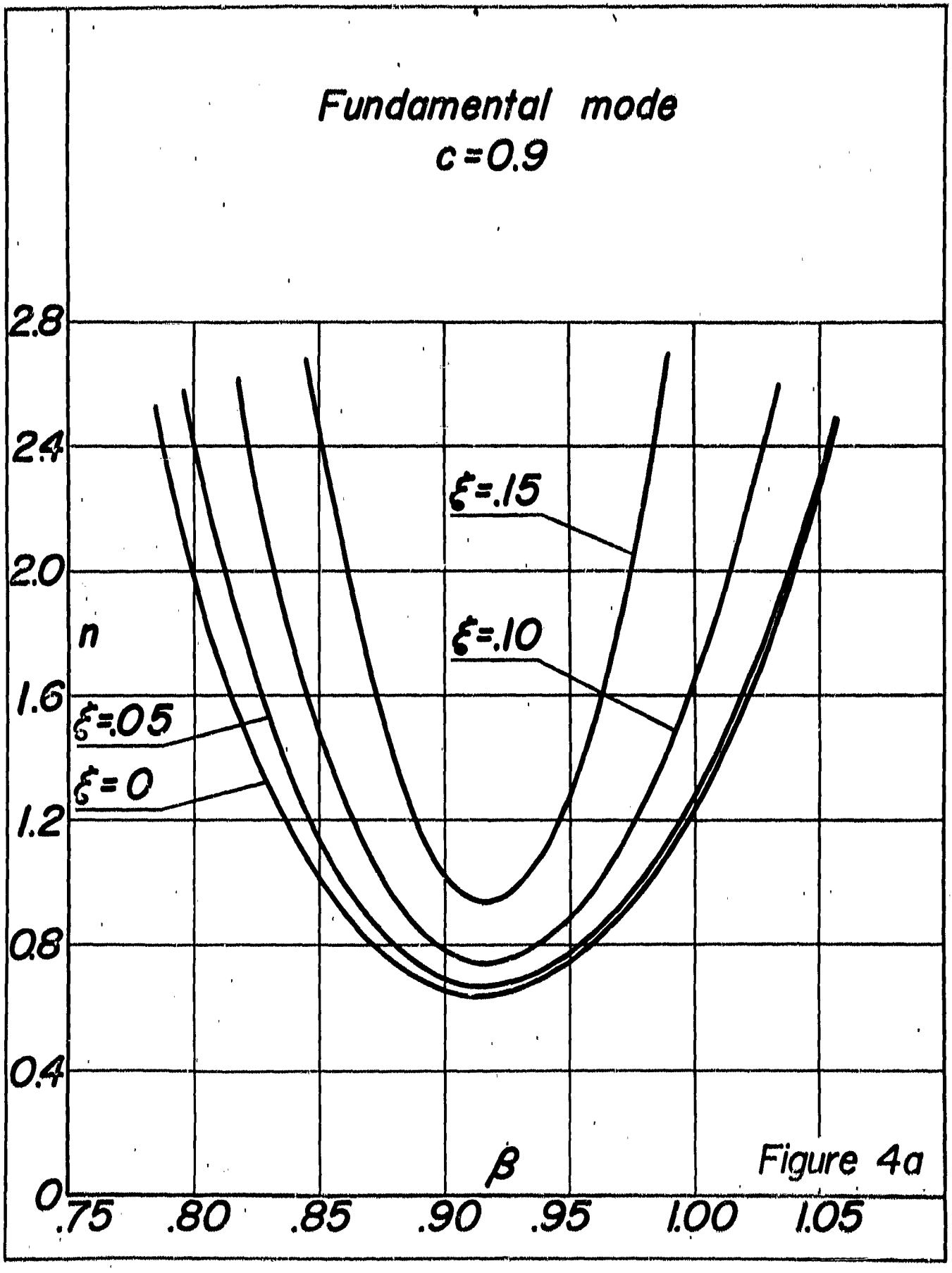
Fundamental mode
c=0.9
2.8
2.4
2.0
1.6
1.2
0.8
0.4
0
n
ξ=.15
ξ=.10
ξ=.05
ξ=0
.75
.80
.85
.90
.95
1.00
1.05
β

Figure 4a

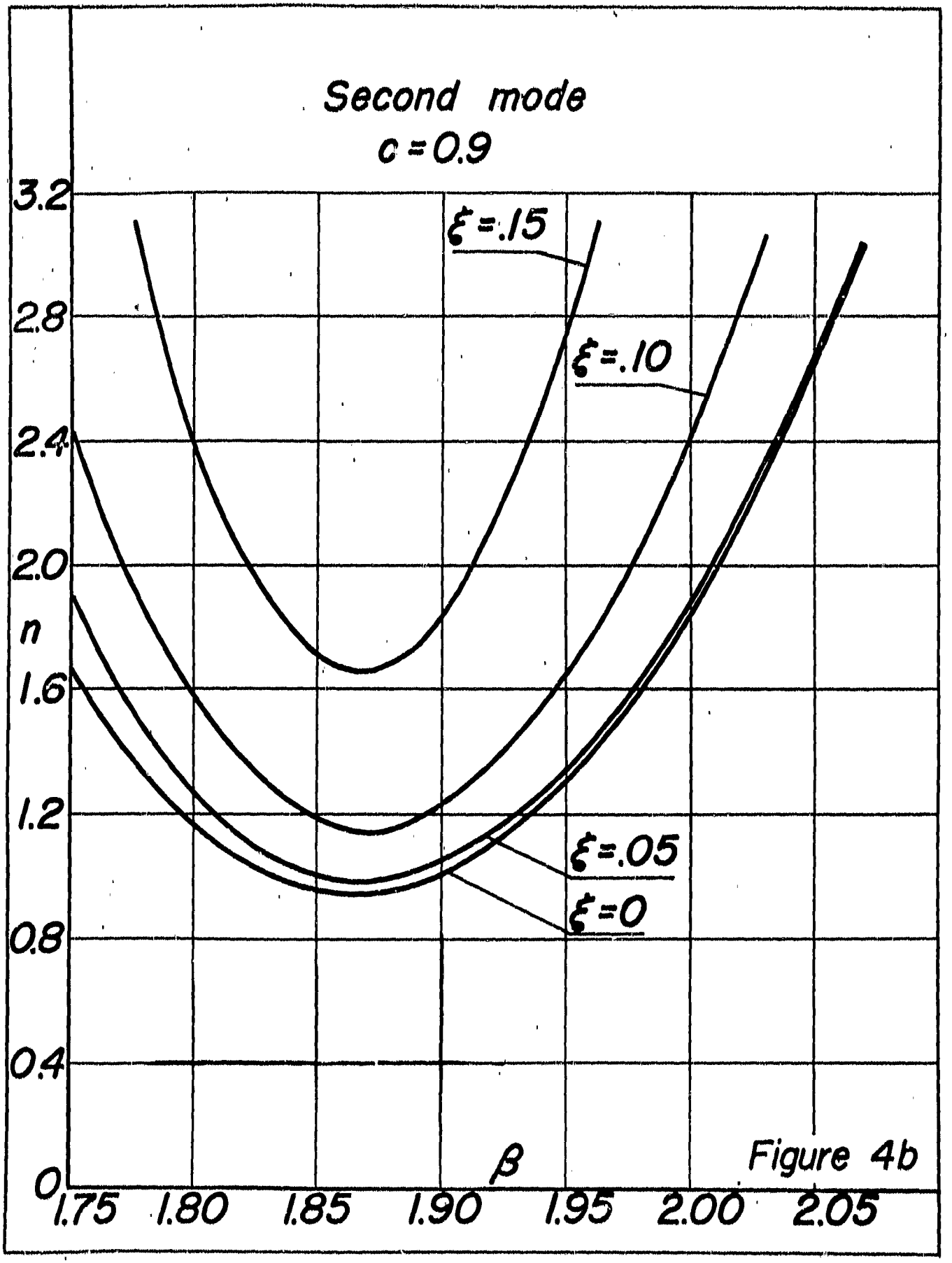
Second mode
c = 0.9
3.2
2.8
2.4
2.0
n
1.6
1.2
0.8
0.4
0
ξ = .15
ξ = .10
ξ = .05
ξ = 0
1.75
1.80
1.85
1.90
1.95
2.00
2.05
β

Figure 4b

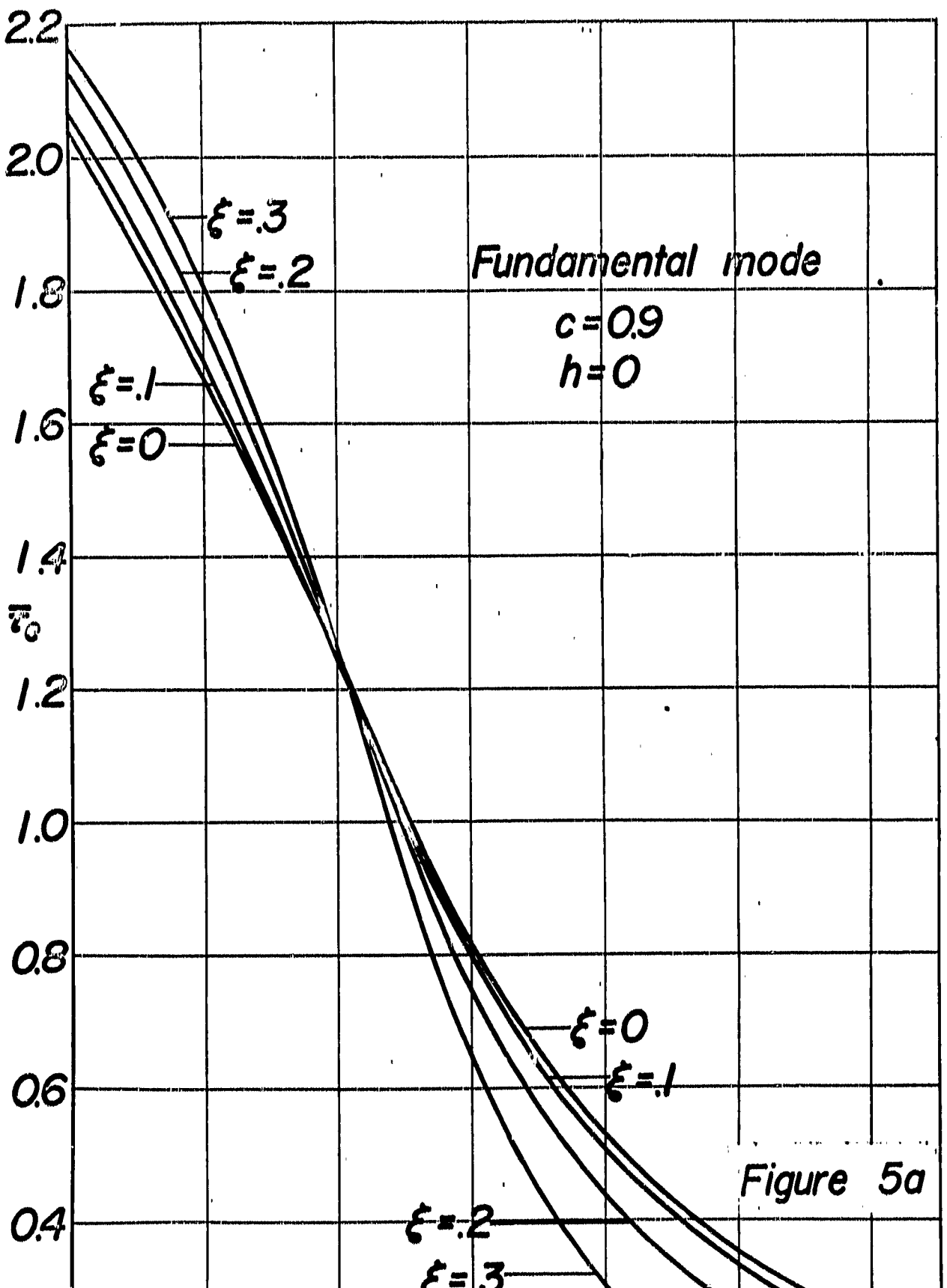
2.2
2.0
1.8
1.6
1.4
1.2
1.0
0.8
0.6
0.4
0.2
T_0
.80
.85
.90
.95
1.00
1.05
1.10
β
ξ=.3
ξ=.2
ξ=.1
ξ=0
Fundamental mode
c=0.9
h=0
ξ=0
ξ=.1
ξ=.2
ξ=.3

Figure 5a

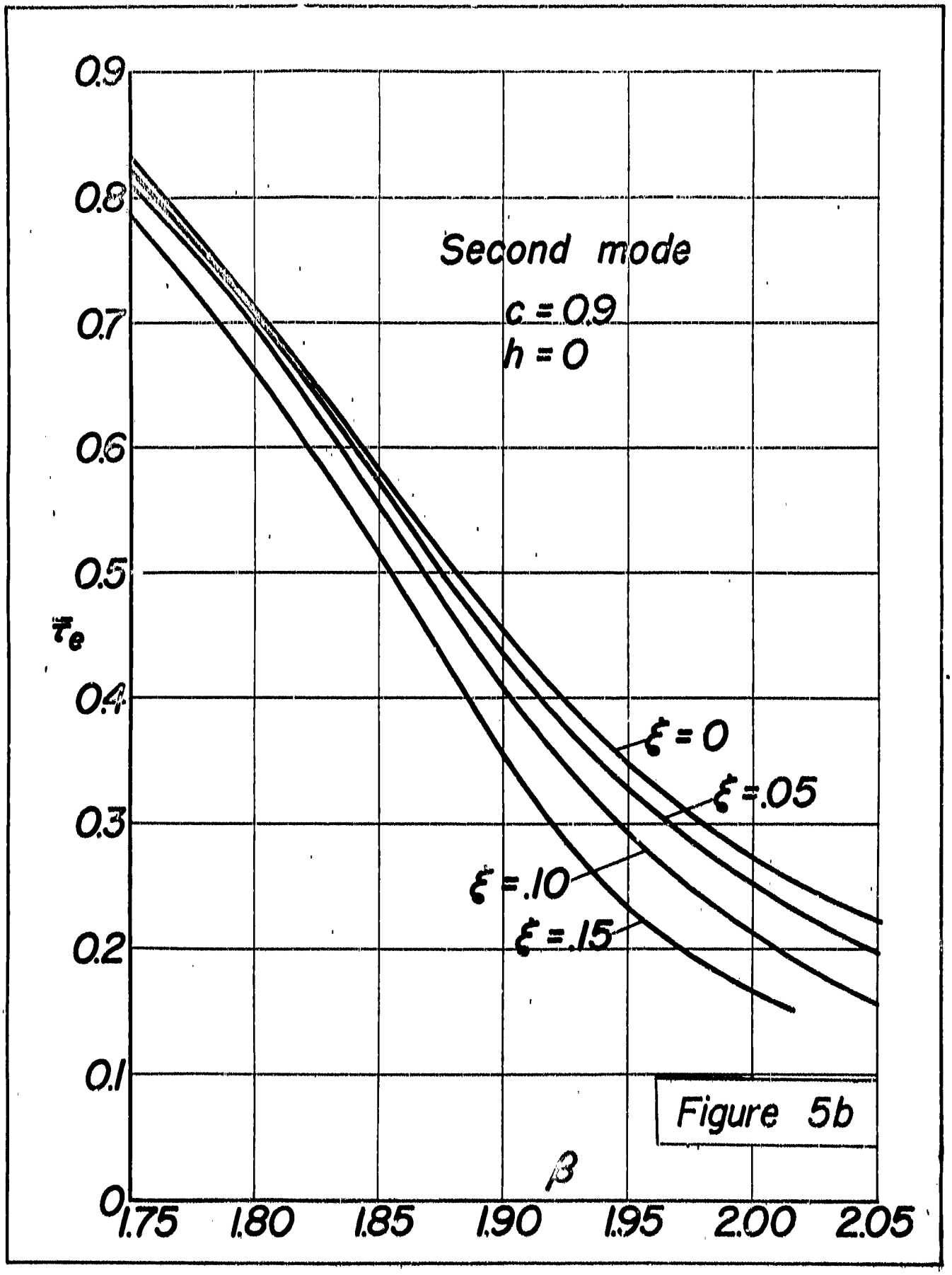
0.9
0.8
0.7
0.6
0.5
$\bar{\tau}_e$
0.4
0.3
0.2
0.1
0
1.75
1.80
1.85
1.90
1.95
2.00
2.05
β
Second mode
c = 0.9
h = 0
ξ = 0
ξ = .05
ξ = .10
ξ = .15

Figure 5b

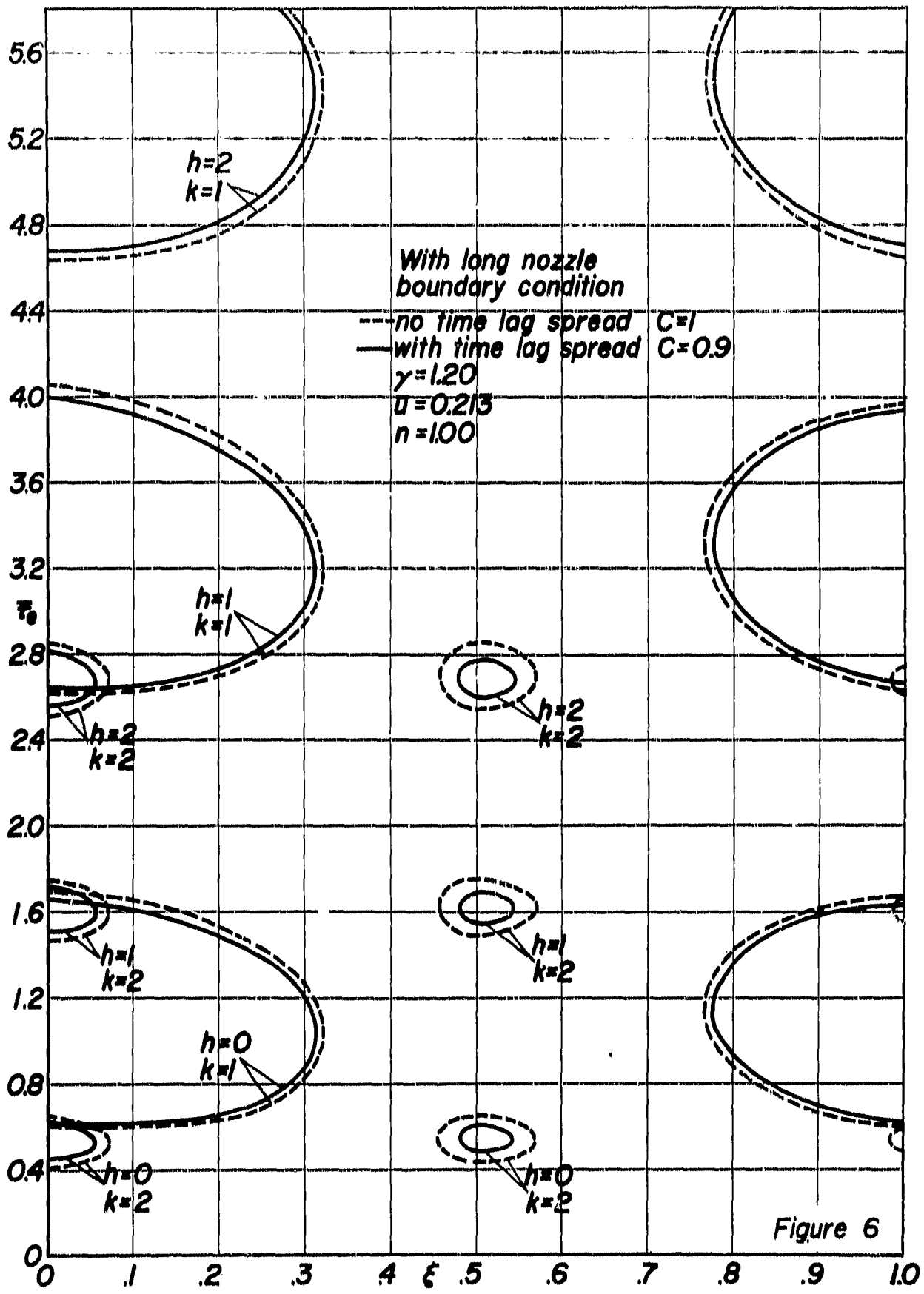
With long nozzle
boundary condition
---no time lag spread C=1
—with time lag spread C=0.9
γ=1.20
u=0.213
n=1.00
h=2
k=1
h=1
k=1
h=2
k=2
h=2
k=2
h=1
k=2
h=1
k=2
h=0
k=1
h=0
k=2
h=0
k=2
η
ξ
0
.1
.2
.3
.4
.5
.6
.7
.8
.9
1.0
0.4
0.8
1.2
1.6
2.0
2.4
2.8
3.2
3.6
4.0
4.4
4.8
5.2
5.6

Figure 6

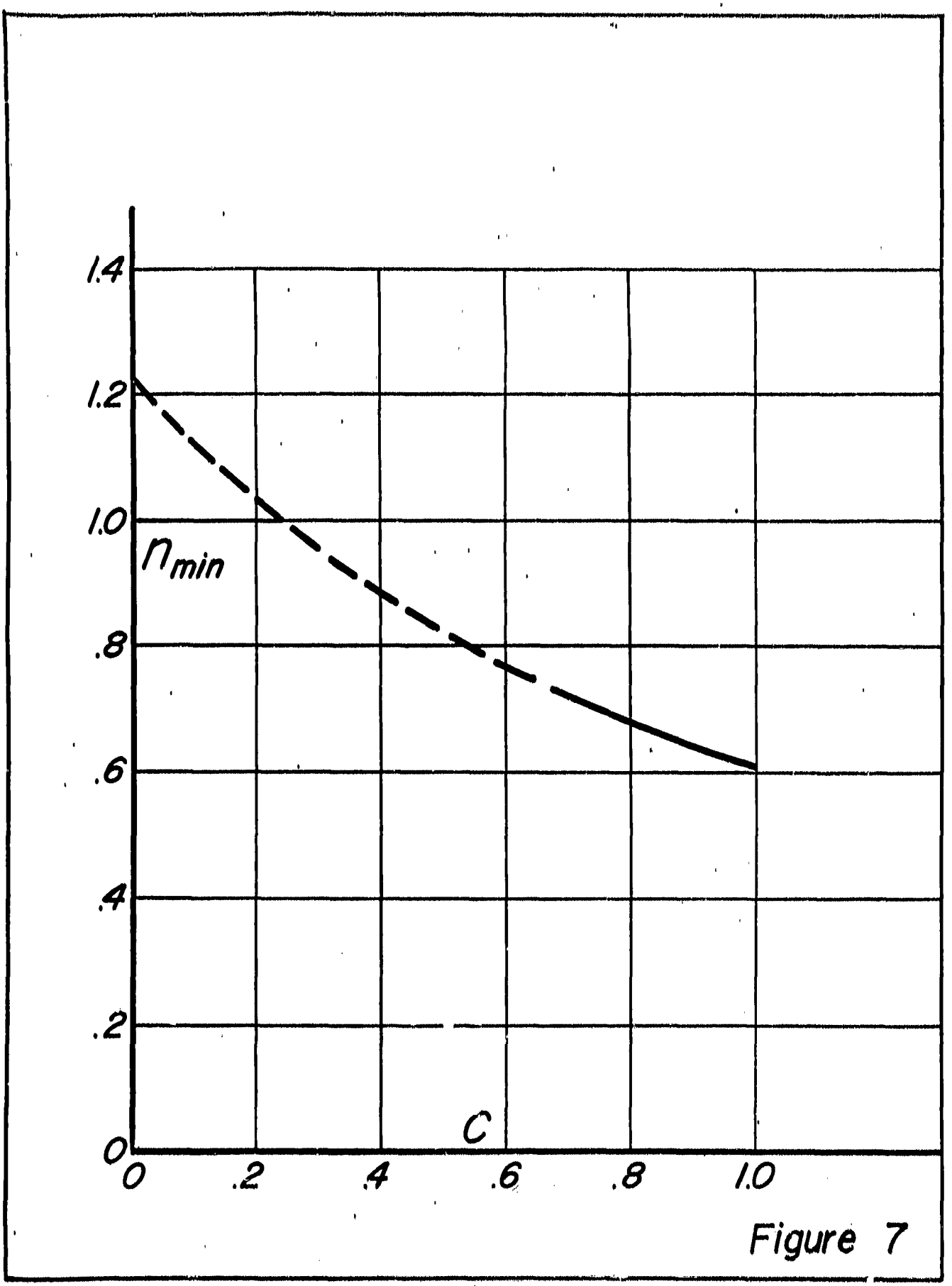

Figure 7

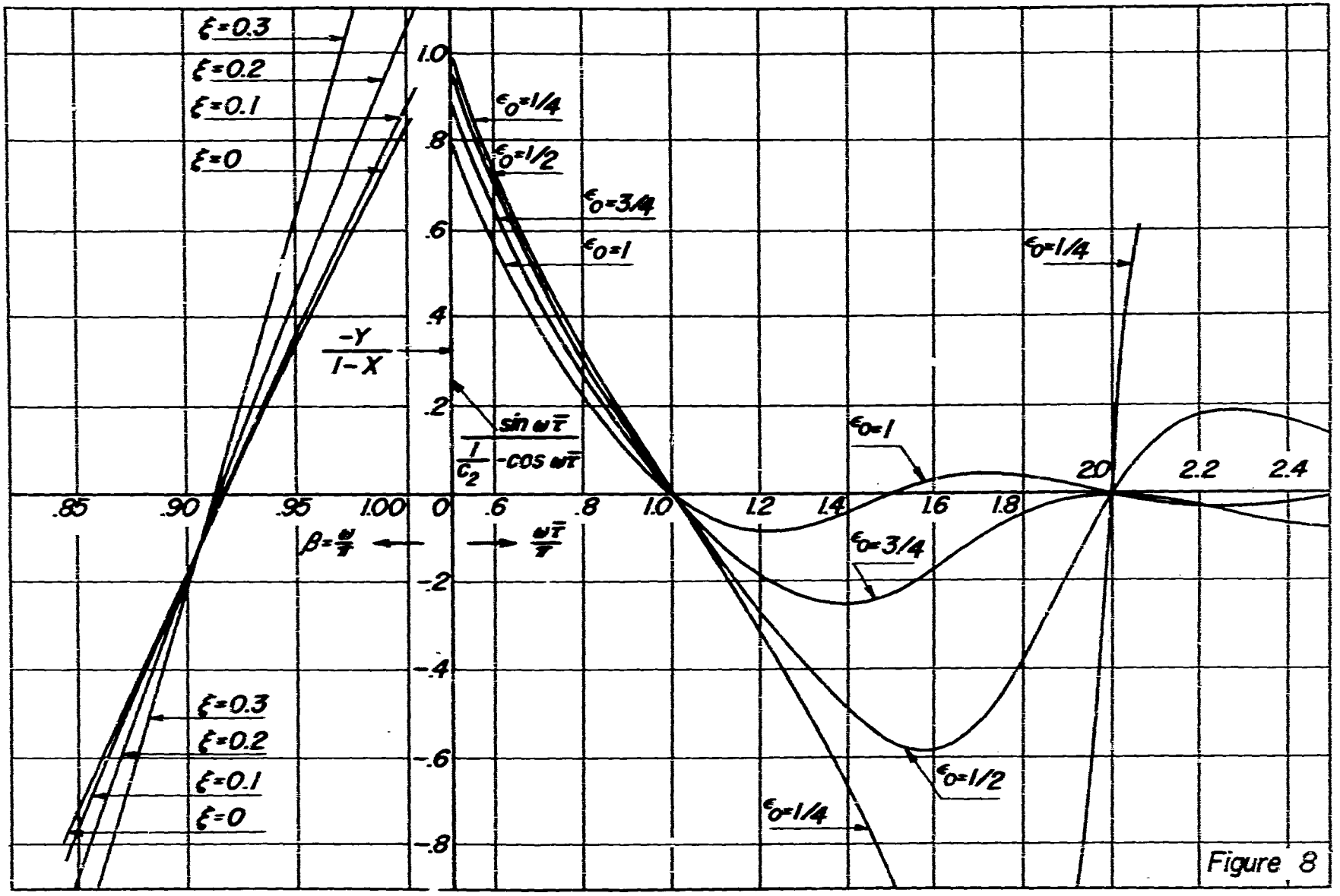
ξ=0.3
ξ=0.2
ξ=0.1
ξ=0
1.0
.8
.6
.4
.2
-Y/1-X
ε0=1/4
ε0=1/2
ε0=3/4
ε0=1
sin ωτ̄ / 1/c2 - cos ωτ̄
.85
.90
.95
1.00
0
.6
.8
1.0
1.2
1.4
1.6
1.8
20
2.2
2.4
β=ω/ν
ωτ̄/ν
-.2
-.4
-.6
-.8
ε0=1/4
ε0=1
ε0=3/4
ε0=1/2
ε0=1/4
ξ=0.3
ξ=0.2
ξ=0.1
ξ=0

Figure 8

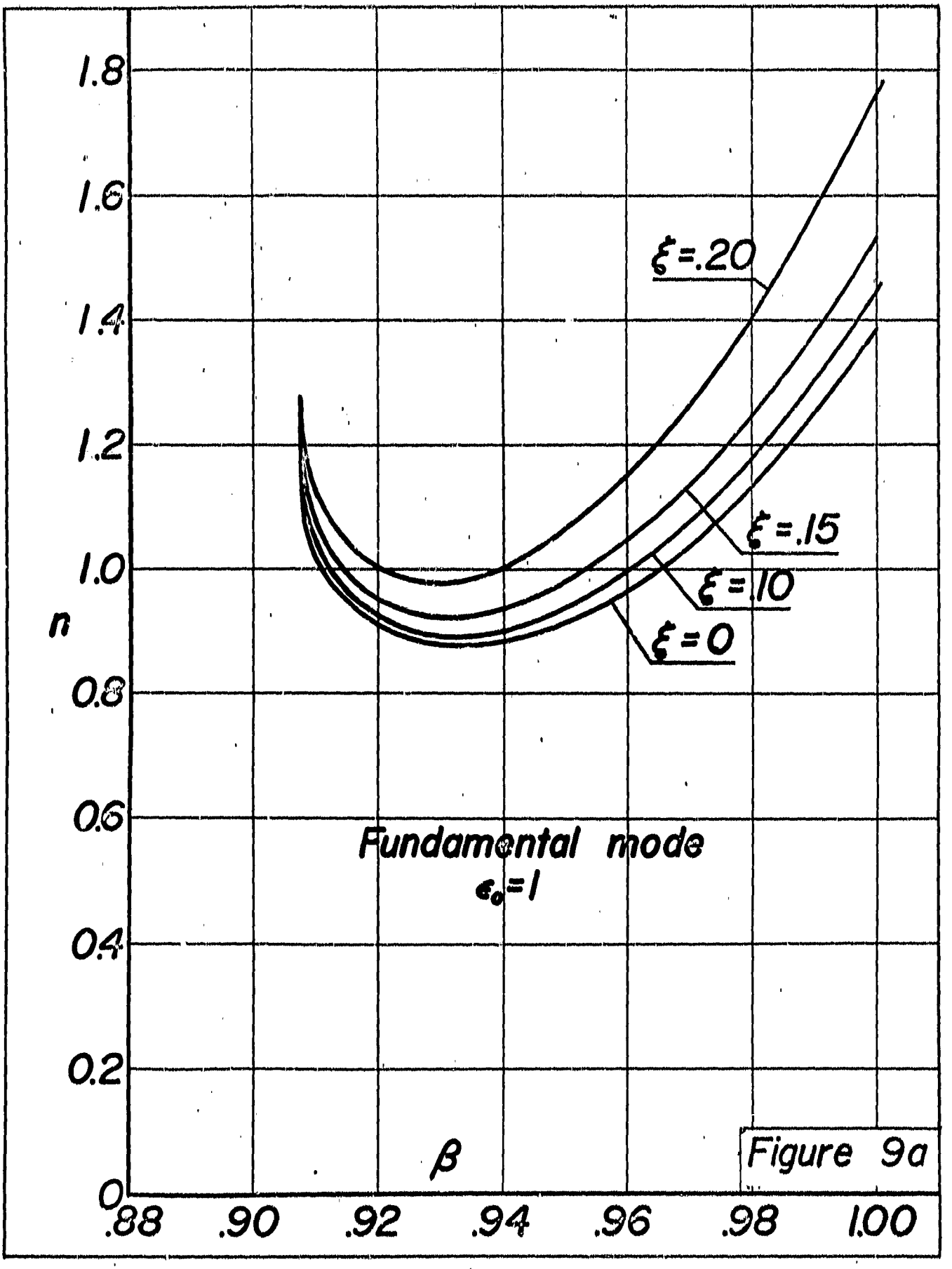
1.8
1.6
1.4
1.2
1.0
0.8
0.6
0.4
0.2
0
n
ξ=.20
ξ=.15
ξ=.10
ξ=0
Fundamental mode
ϵ_0=1
β
.88
.90
.92
.94
.96
.98
1.00

Figure 9a

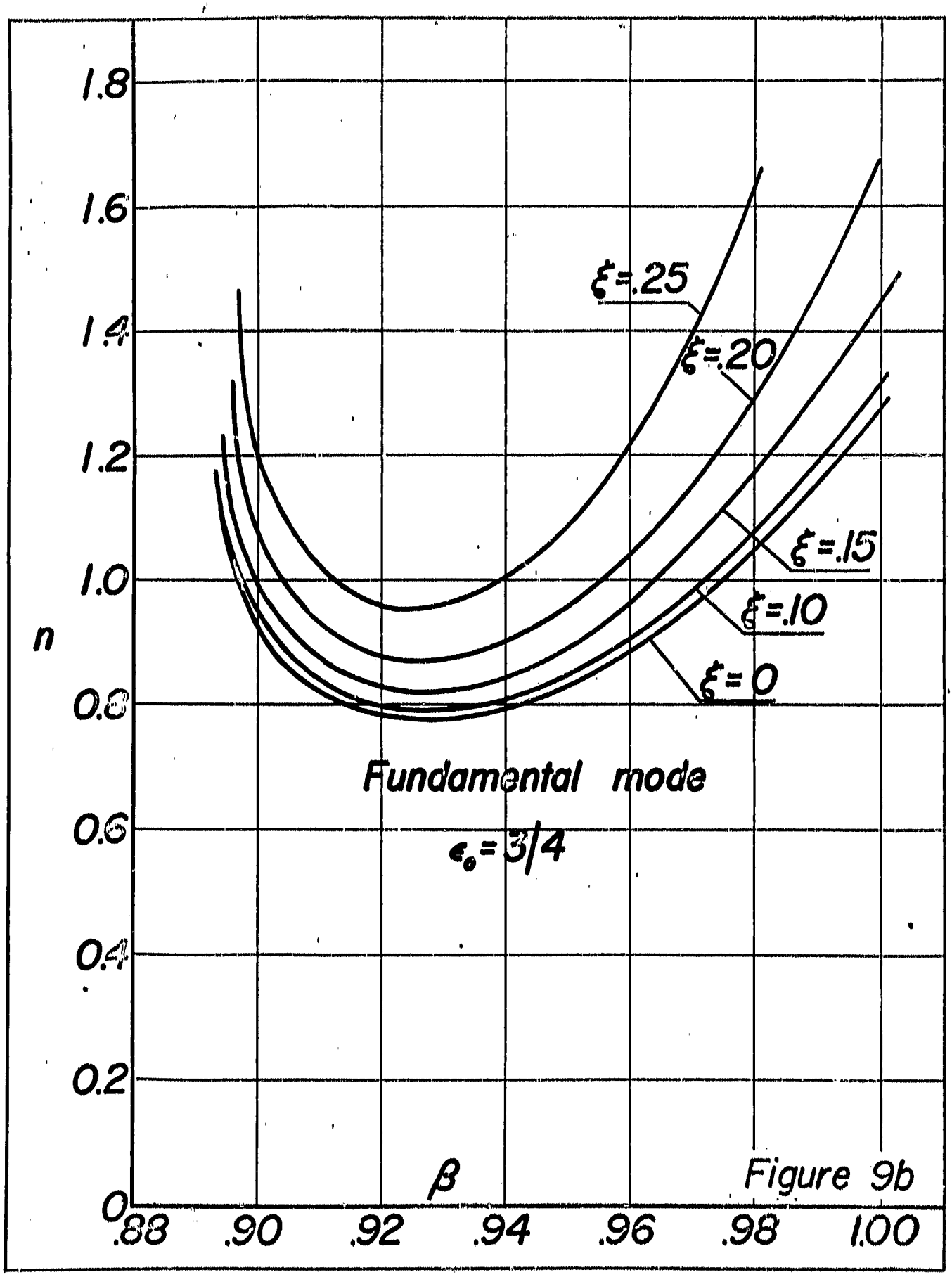
1.8
1.6
1.4
1.2
1.0
0.8
0.6
0.4
0.2
0
n
ξ=.25
ξ=.20
ξ=.15
ξ=.10
ξ=0
Fundamental mode
$\epsilon_0 = 3/4$
.88
.90
.92
.94
.96
.98
1.00
β

Figure 9b

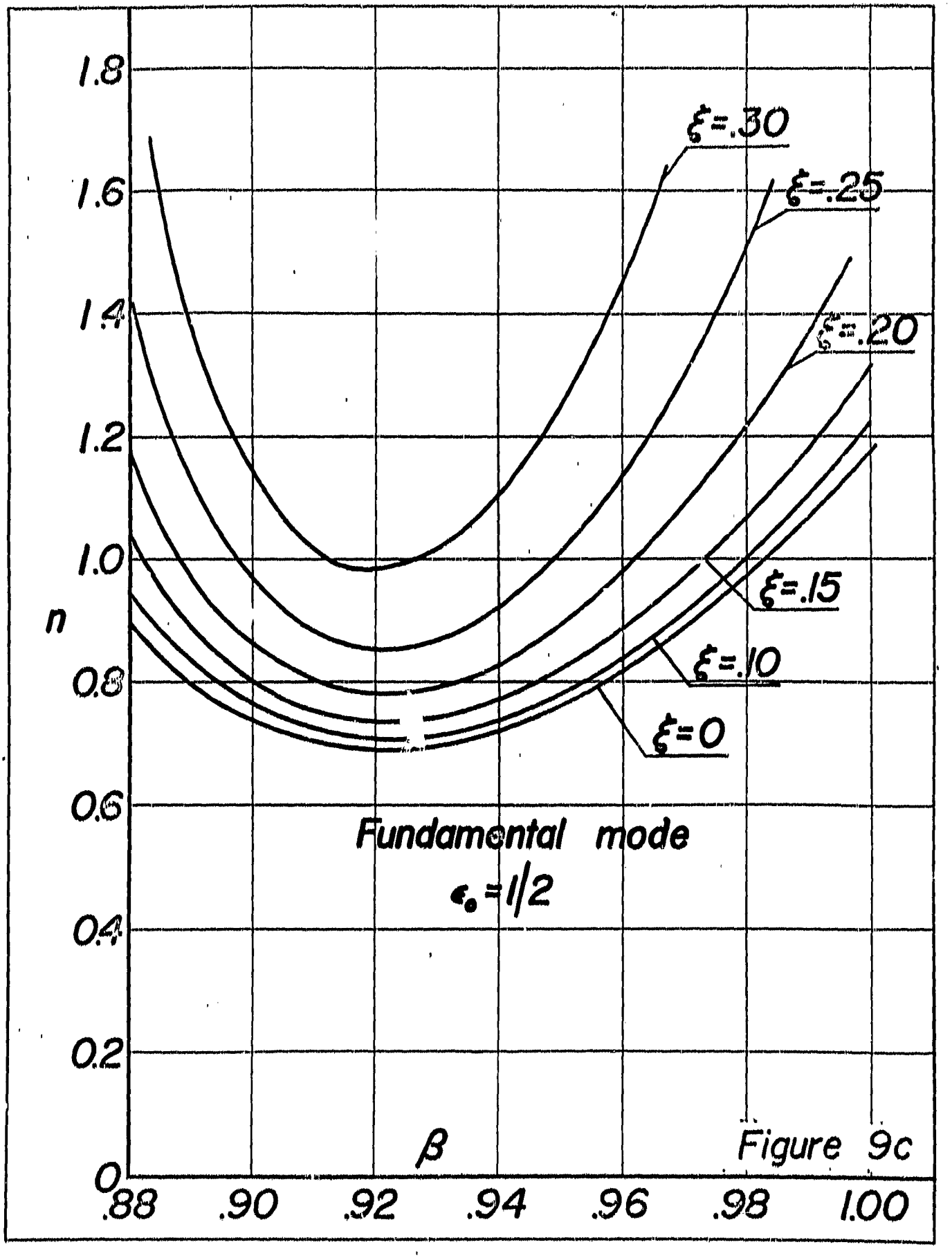
1.8
1.6
1.4
1.2
1.0
0.8
0.6
0.4
0.2
0
n
ξ=.30
ξ=.25
ξ=.20
ξ=.15
ξ=.10
ξ=0
Fundamental mode
$\epsilon_0 = 1/2$
.88
.90
.92
.94
.96
.98
1.00
β

Figure 9c

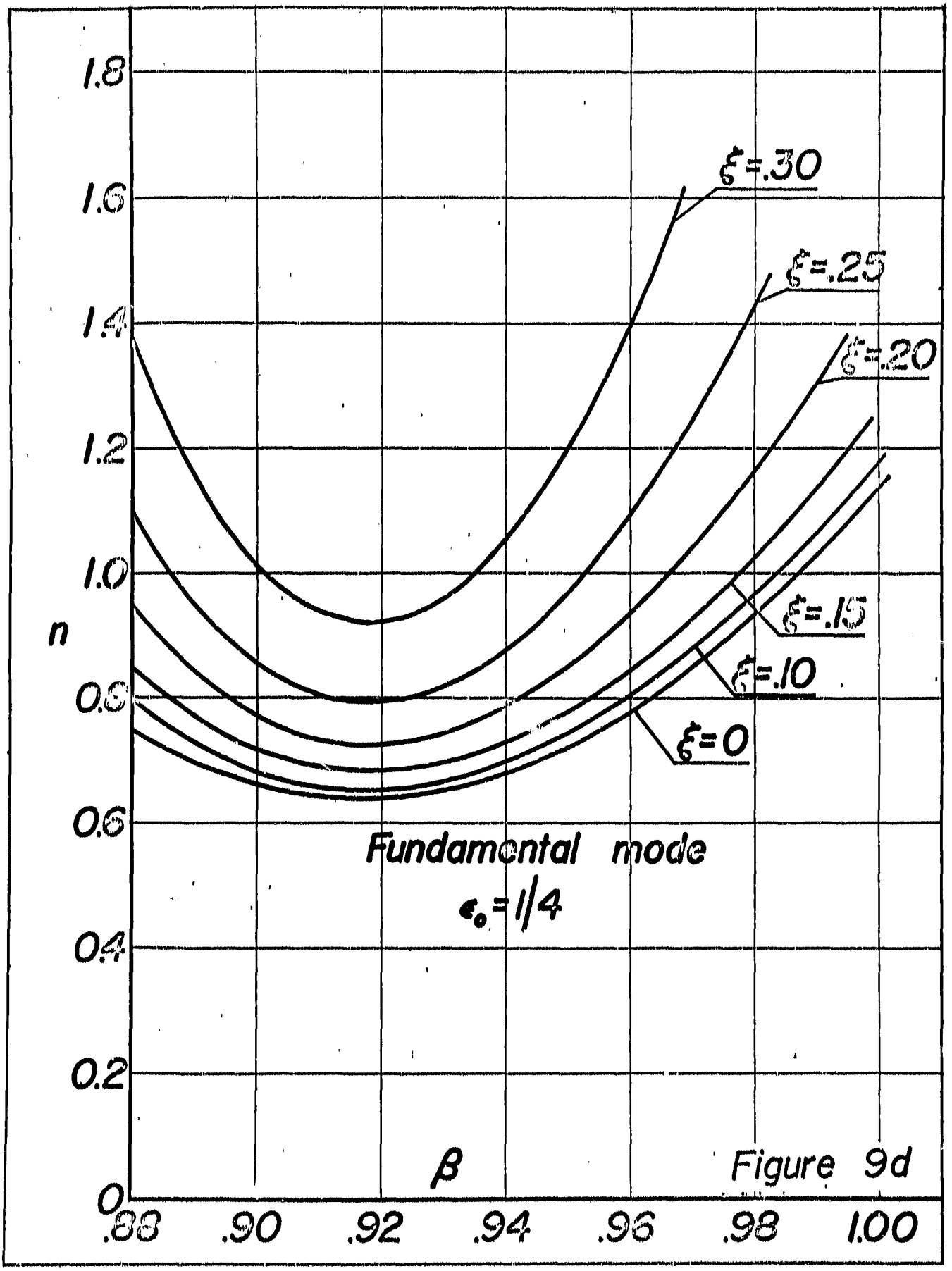
1.8
1.6
1.4
1.2
1.0
0.8
0.6
0.4
0.2
0
n
ξ=.30
ξ=.25
ξ=.20
ξ=.15
ξ=.10
ξ=0
Fundamental mode
$\epsilon_0 = 1/4$
.88
.90
.92
.94
.96
.98
1.00
β

Figure 9d

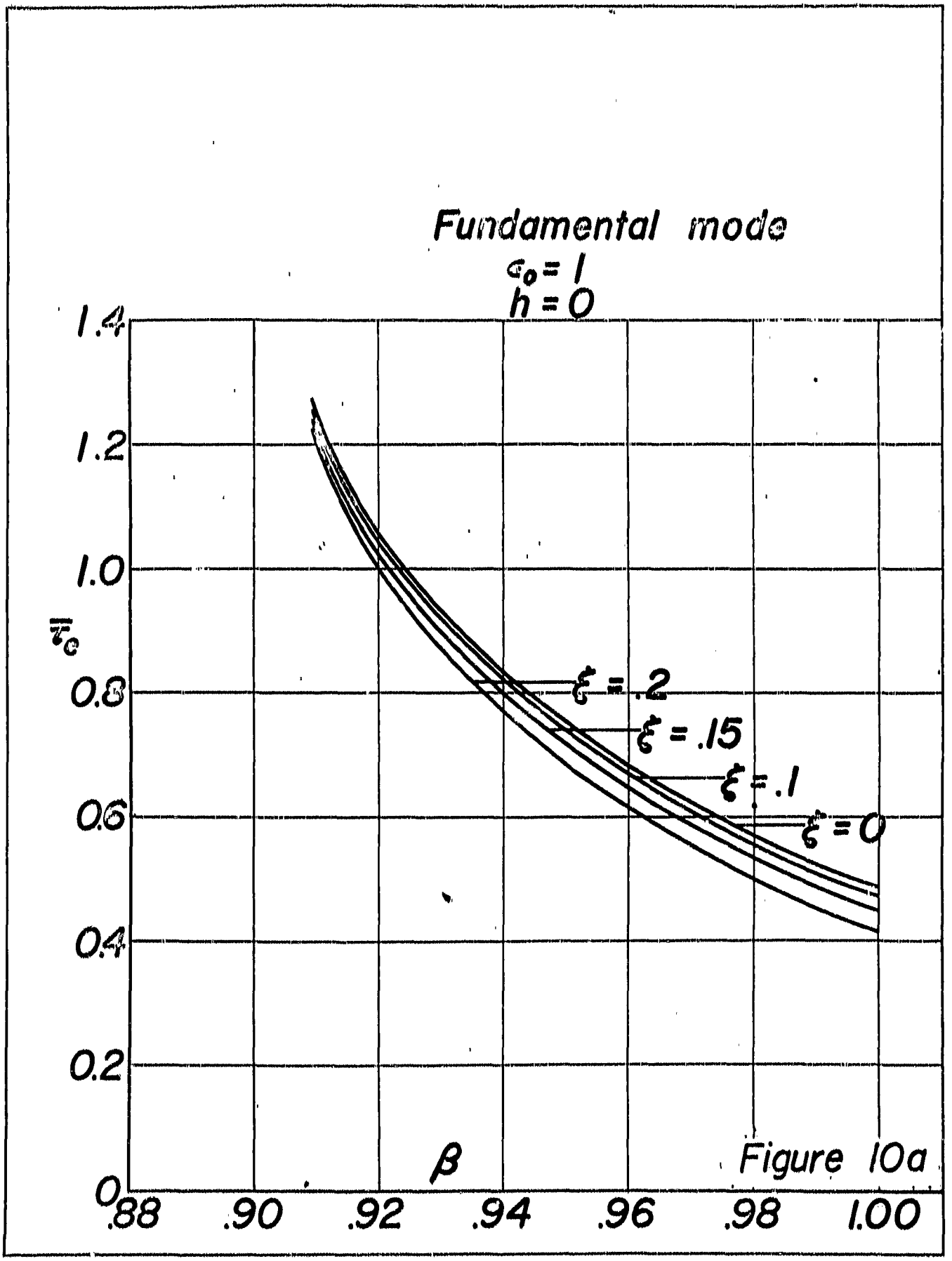
Fundamental mode
$c_o = 1$
$h = 0$
1.4
1.2
1.0
$\bar{c}_c$
0.8
0.6
0.4
0.2
0
$\xi = .2$
$\xi = .15$
$\xi = .1$
$\xi = 0$
β
.88
.90
.92
.94
.96
.98
1.00

Figure 10a

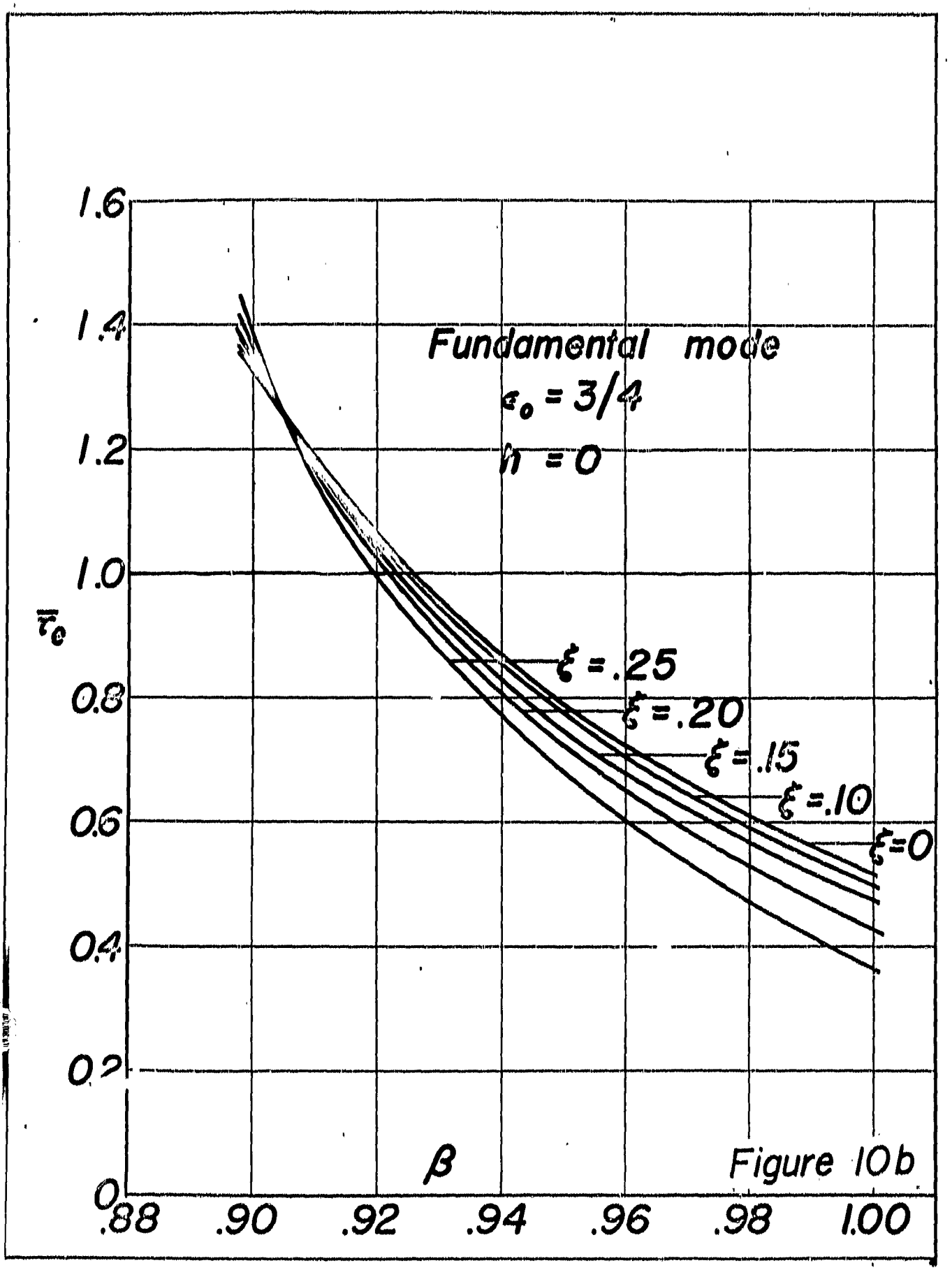
Fundamental mode
$\epsilon_0 = 3/4$
$\eta = 0$
$\bar{r}_e$
$\xi = .25$
$\xi = .20$
$\xi = .15$
$\xi = .10$
$\xi = 0$
β
1.6
1.4
1.2
1.0
0.8
0.6
0.4
0.2
0
.88
.90
.92
.94
.96
.98
1.00

Figure 10b

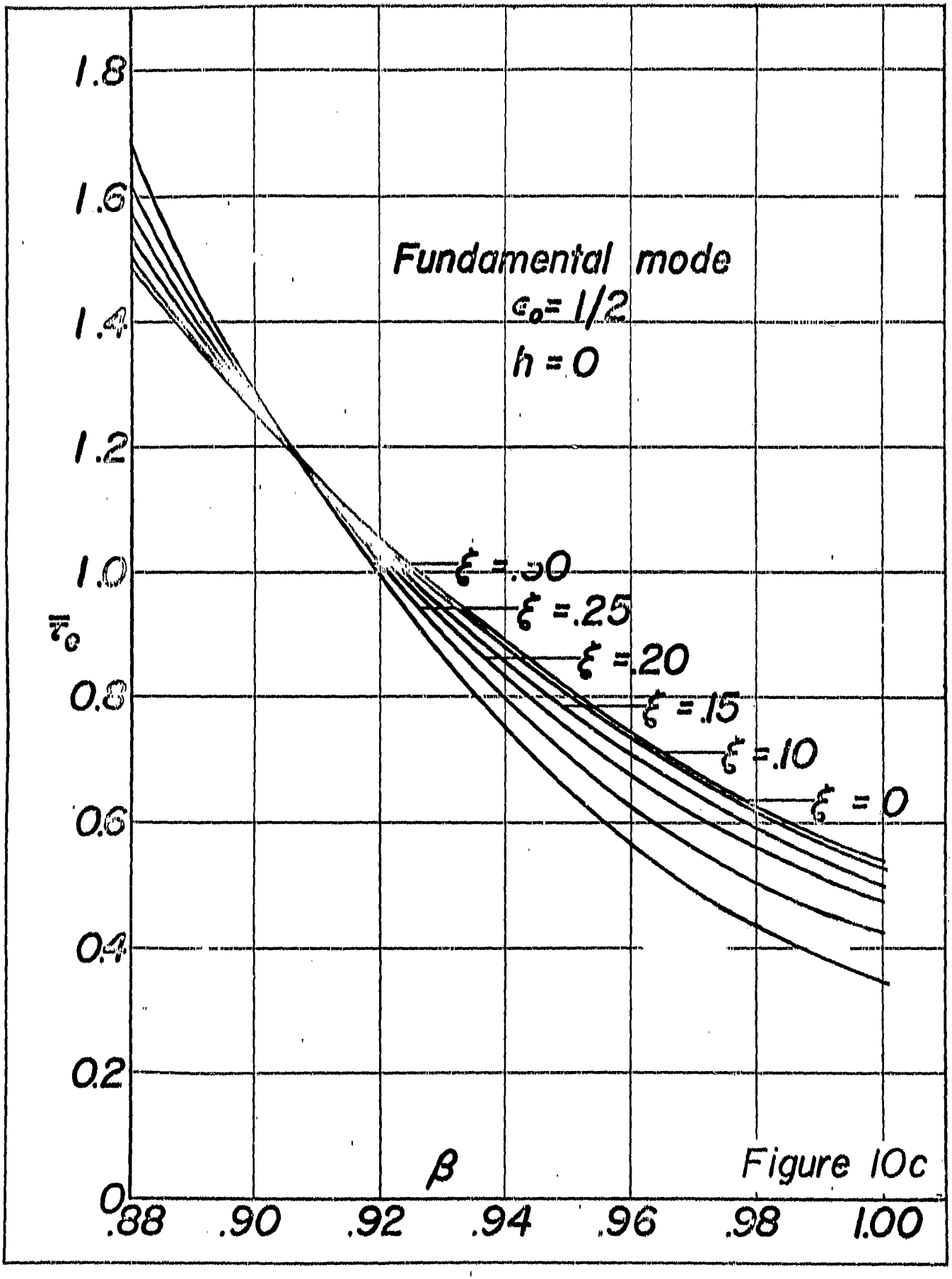
1.8
1.6
1.4
1.2
1.0
0.8
0.6
0.4
0.2
0
$\bar{r}_c$
Fundamental mode
$c_o = 1/2$
$h = 0$
$\xi = .30$
$\xi = .25$
$\xi = .20$
$\xi = .15$
$\xi = .10$
$\xi = 0$
.88
.90
.92
.94
.96
.98
1.00
β

Figure 10c

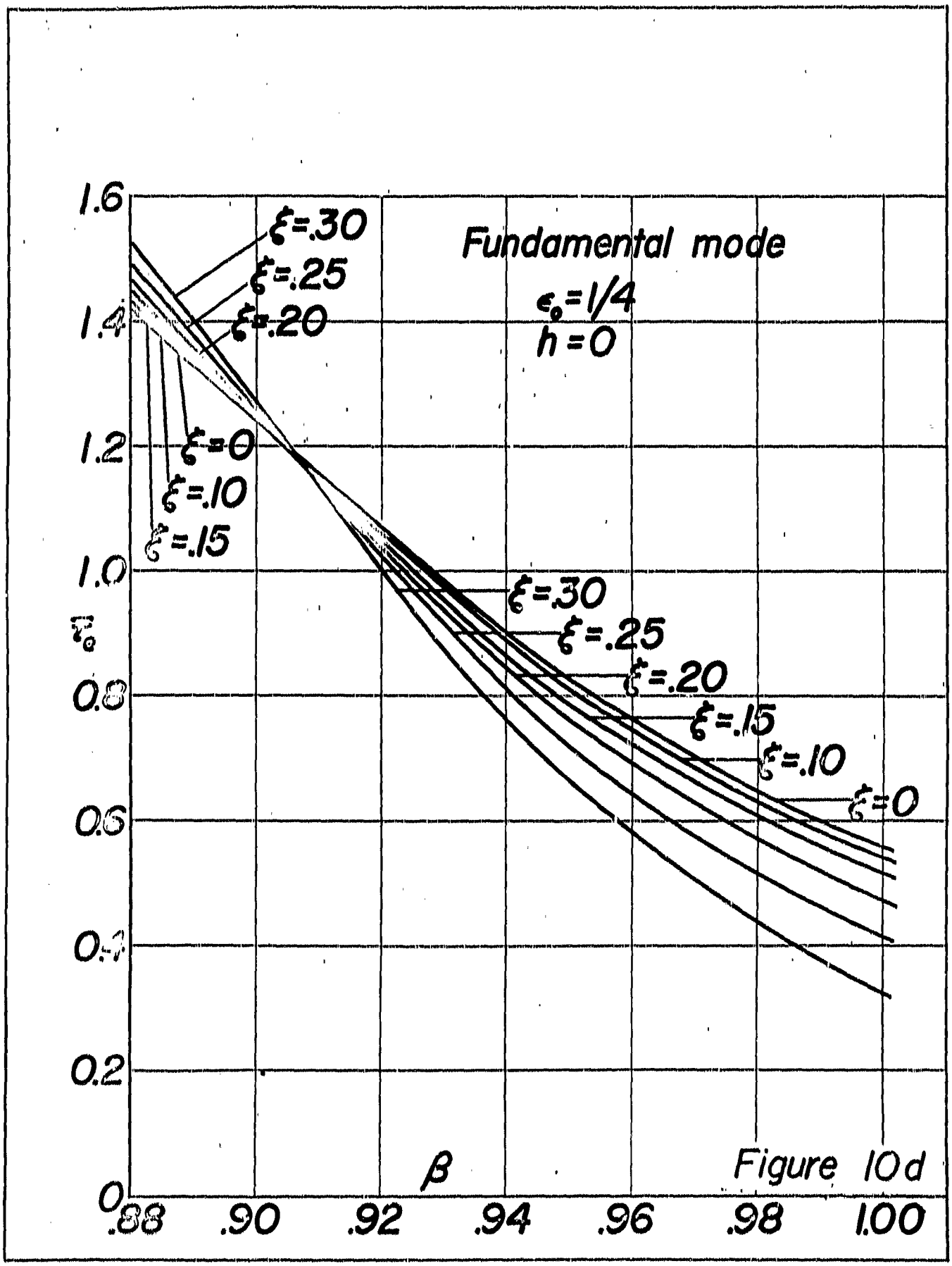
Fundamental mode
$\epsilon_0 = 1/4$
$h = 0$
$\xi = .30$
$\xi = .25$
$\xi = .20$
$\xi = 0$
$\xi = .10$
$\xi = .15$
$\xi = .30$
$\xi = .25$
$\xi = .20$
$\xi = .15$
$\xi = .10$
$\xi = 0$
$\bar{r}_0$
β
1.6
1.4
1.2
1.0
0.8
0.6
0.4
0.2
0
.88
.90
.92
.94
.96
.98
1.00

Figure 10d

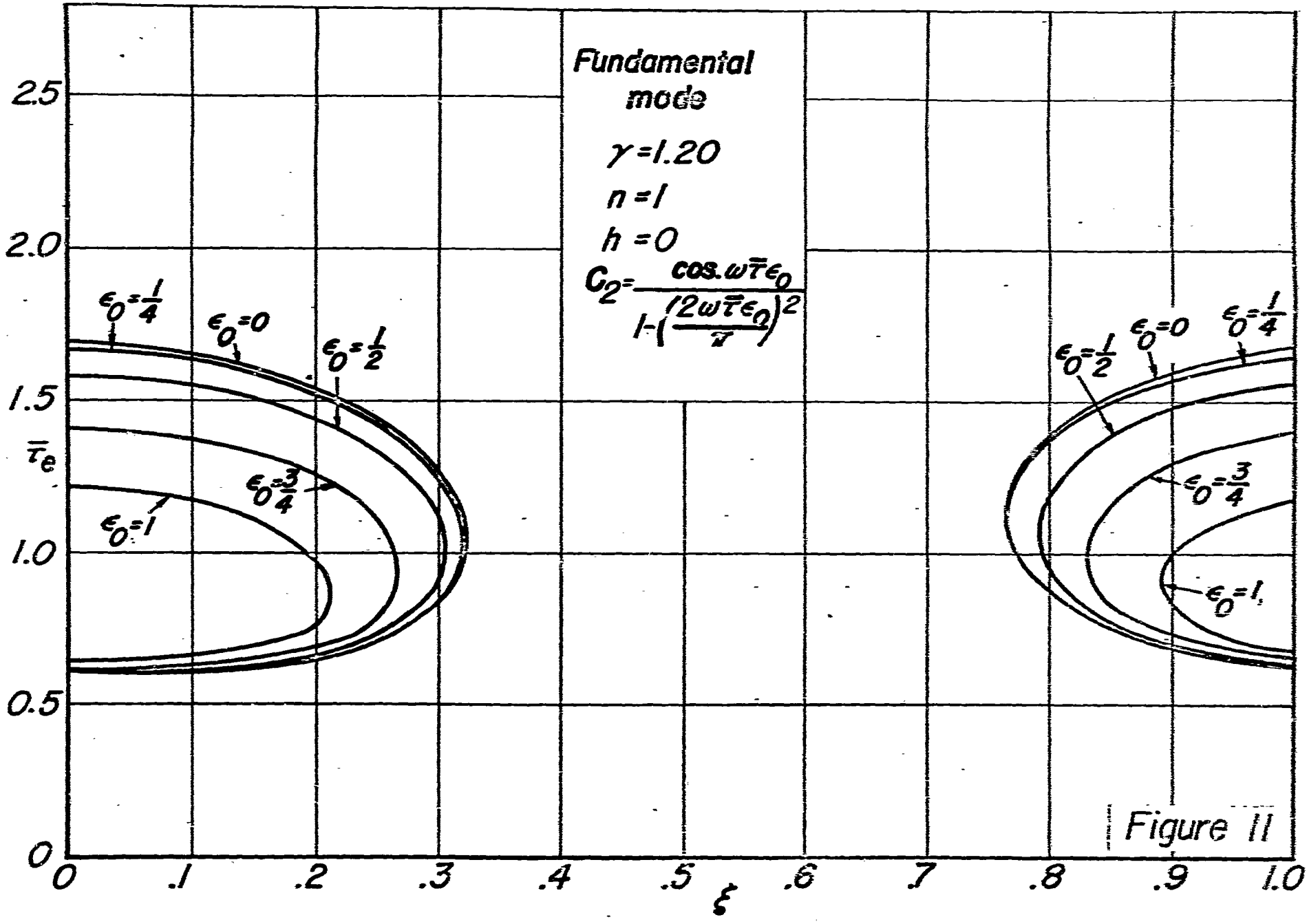
Fundamental mode
γ=1.20
n=1
h=0
$C_2=\frac{\cos.\omega\bar{\tau}\epsilon_0}{1-\left(\frac{2\omega\bar{\tau}\epsilon_0}{\pi}\right)^2}$
$\epsilon_0=\frac{1}{4}$
$\epsilon_0=0$
$\epsilon_0=\frac{1}{2}$
$\epsilon_0=\frac{3}{4}$
$\epsilon_0=1$
$\bar{\tau}_e$
ξ
0
0.5
1.0
1.5
2.0
2.5
.1
.2
.3
.4
.5
.6
.7
.8
.9
1.0

Figure 11

$$C_1 = \frac{\sin \omega \bar{\tau} \epsilon_0}{\omega \bar{\tau} \epsilon_0} \qquad C_2 = \frac{\cos \omega \bar{\tau} \epsilon_0}{1 - \left(\frac{2\omega \bar{\tau} \epsilon_0}{\pi}\right)^2}$$

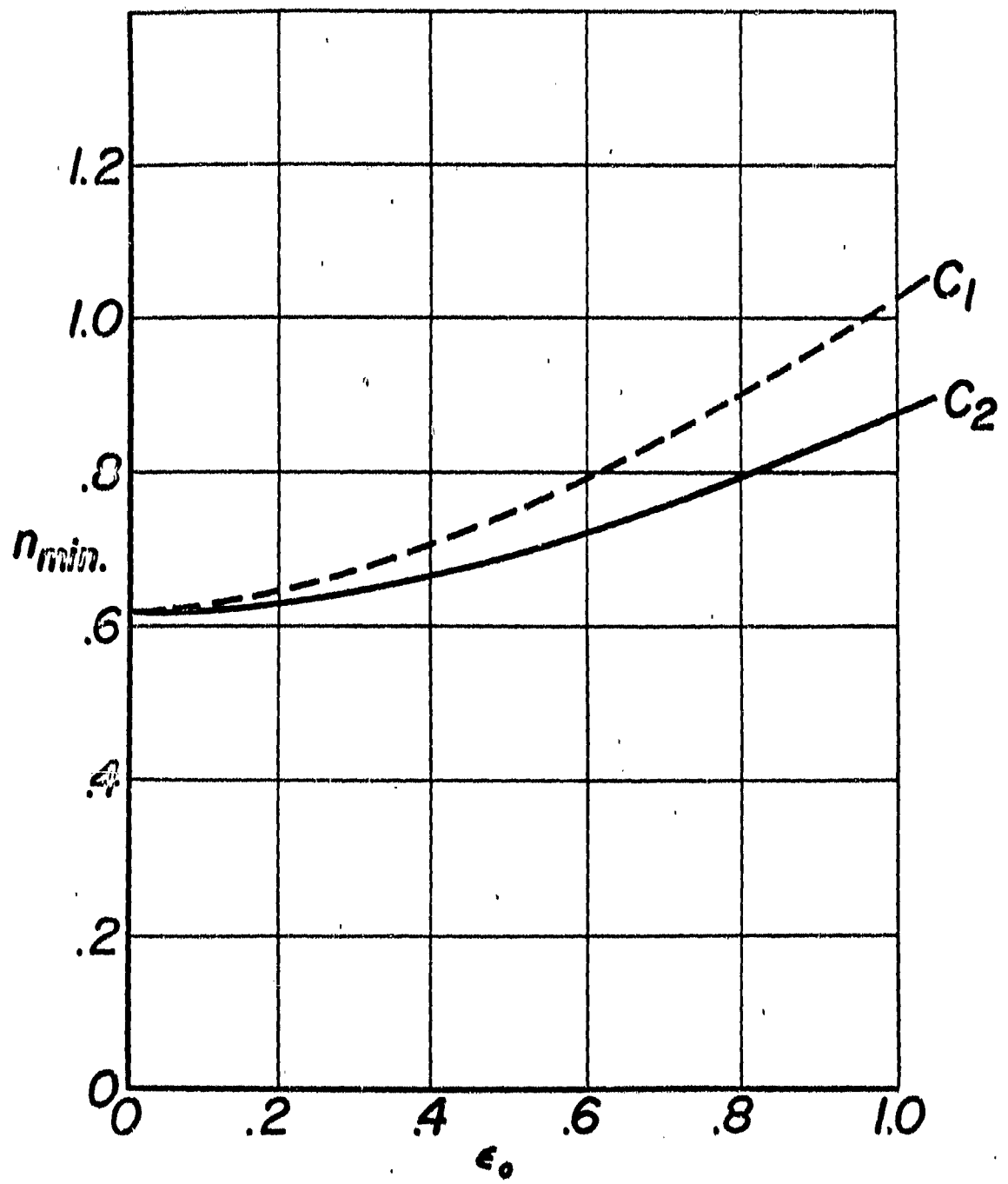

Figure 12

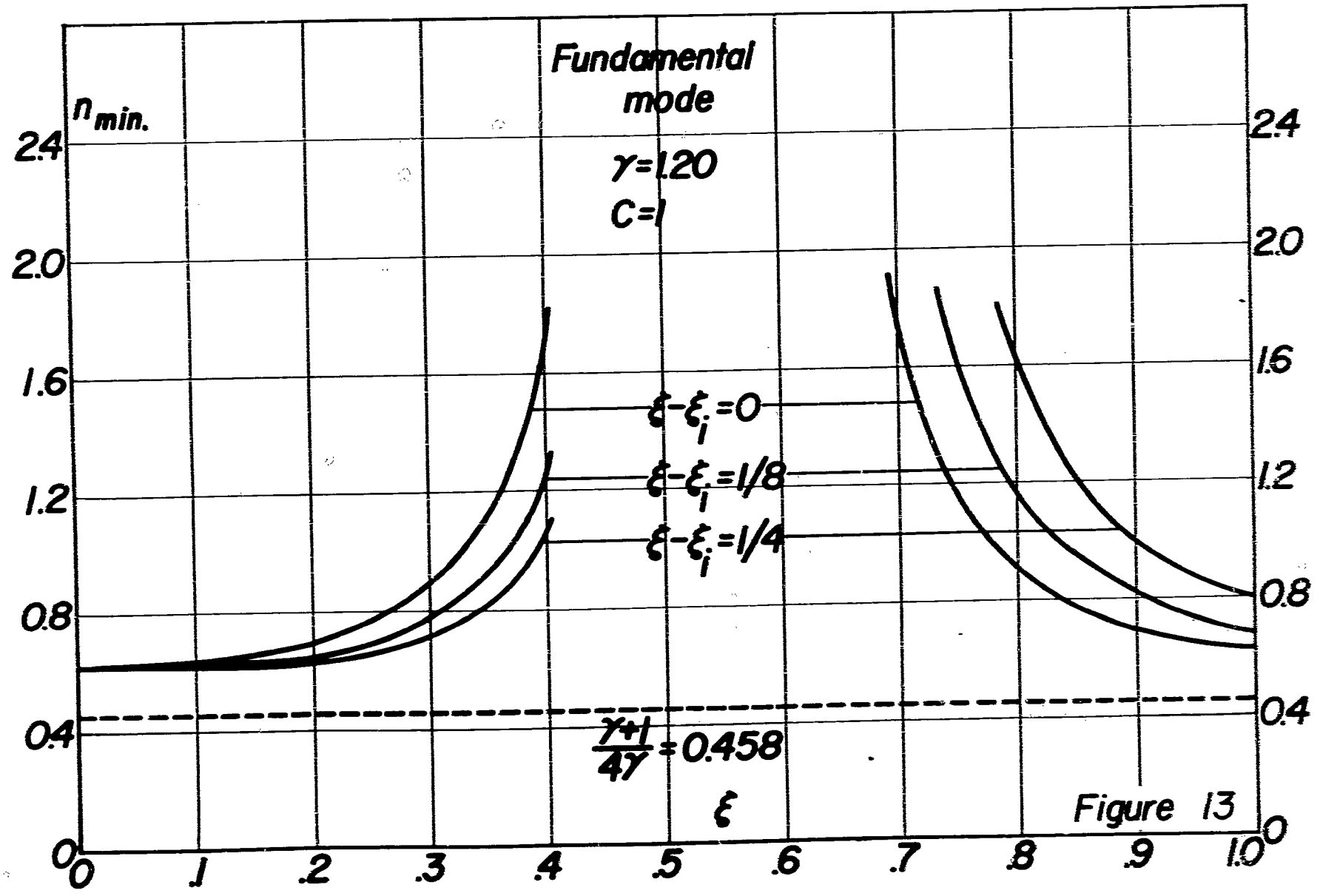
Fundamental mode
$\gamma = 1.20$
$C = 1$
$\eta_{min.}$
$\xi - \xi_i = 0$
$\xi - \xi_i = 1/8$
$\xi - \xi_i = 1/4$
$\frac{\gamma+1}{4\gamma} = 0.458$
ξ
0
.1
.2
.3
.4
.5
.6
.7
.8
.9
1.0
0.4
0.8
1.2
1.6
2.0
2.4

Figure 13

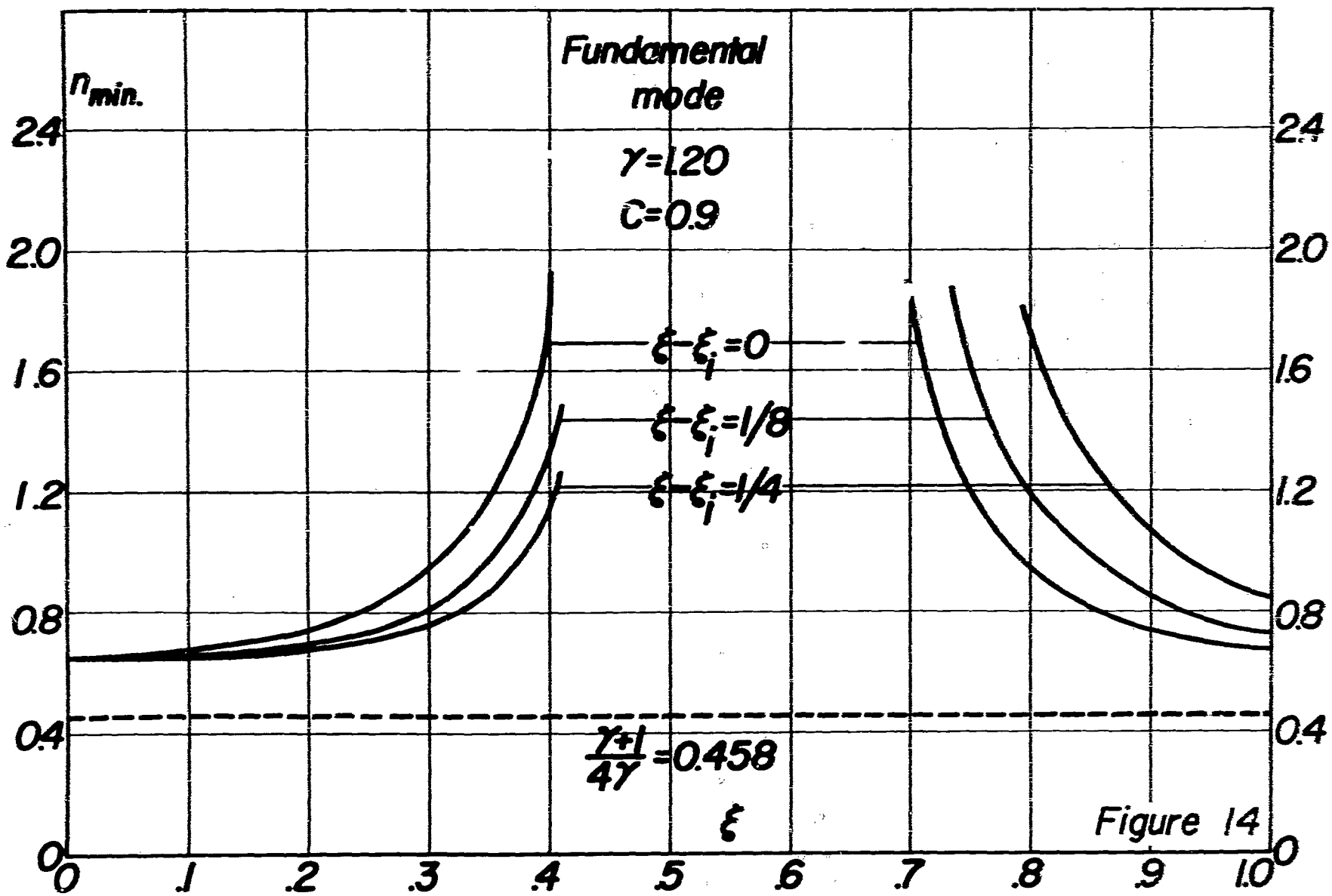
Fundamental mode
γ=1.20
C=0.9
$\eta_{min.}$
$\epsilon-\xi_i=0$
$\epsilon-\xi_i=1/8$
$\epsilon-\xi_i=1/4$
$\frac{\gamma+1}{4\gamma}=0.458$
ϵ
0
.1
.2
.3
.4
.5
.6
.7
.8
.9
1.0
0.4
0.8
1.2
1.6
2.0
2.4

Figure 14

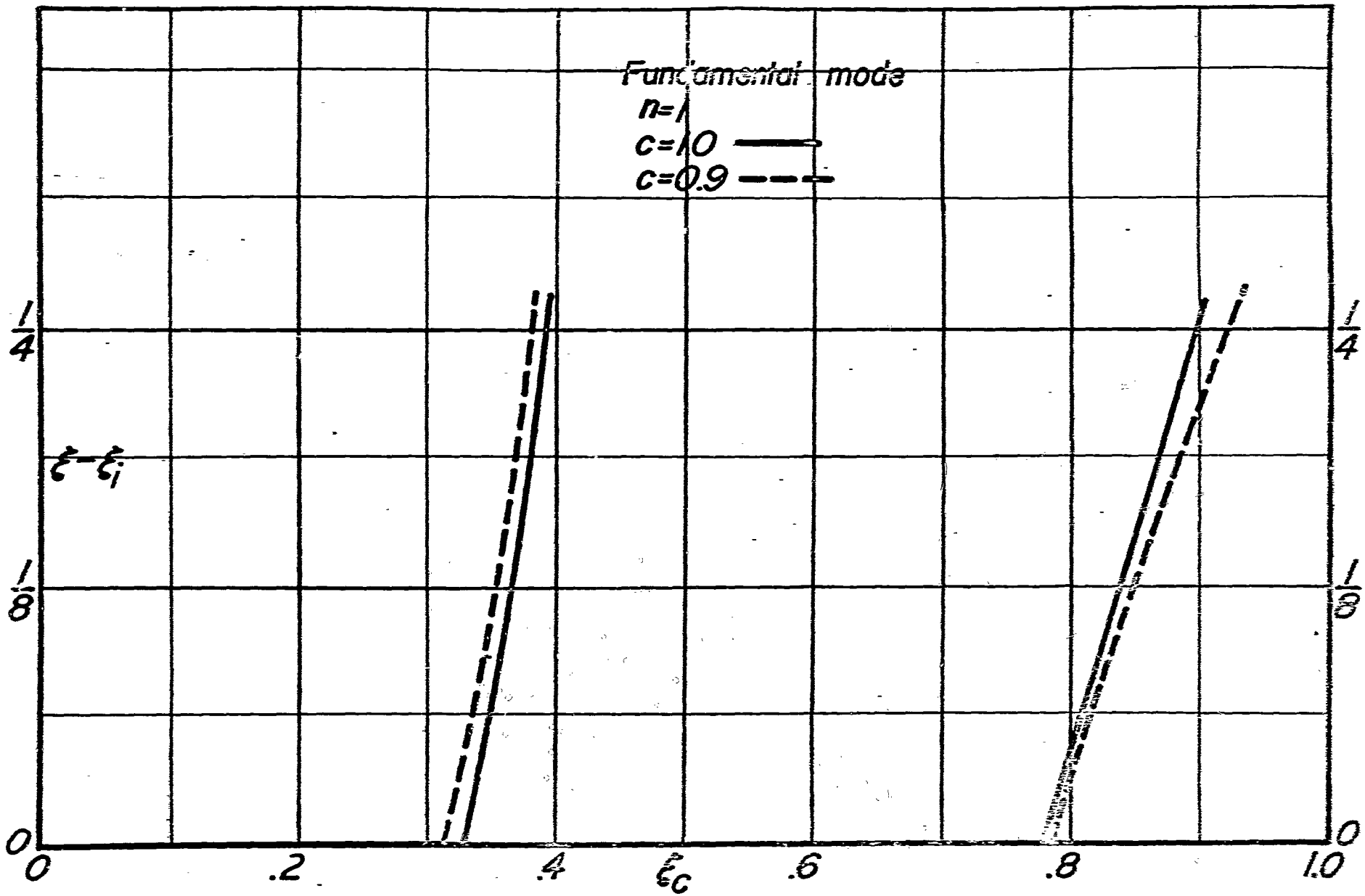

Figure 15